

AD-A008 521

REMOTE DETECTION OF THE HYDRONIUM ION

Stanley M. Klainer

Block Engineering, Incorporated

Prepared for:

Rome Air Development Center

March 1975

DISTRIBUTED BY:

NTIS

National Technical Information Service
U. S. DEPARTMENT OF COMMERCE

This report has been reviewed by the RADC Information Office (OI) and is releasable to the National Technical Information Service (NTIS). At NTIS it will be available to the general public, including foreign nations.

This technical report has been reviewed and is approved for publication.

APPROVED:




DONALD D. DYLLIS
Project Engineer

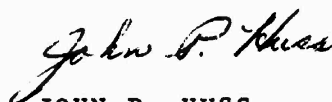
APPROVED:



HOWARD DAVIS
Technical Director
Intel & Recon Division

| | |
|---|-------------------------------------|
| APPROVED BY | |
| NTIS | <input checked="" type="checkbox"/> |
| DTIC | <input checked="" type="checkbox"/> |
| UNCLASSIFIED | <input checked="" type="checkbox"/> |
| BY | |
| DATE | |
|  | |

FOR THE COMMANDER:



JOHN P. HUSS
Acting Chief, Plans Office

This effort was funded totally by the Laboratory Directors' Fund.

Do not return this copy; retain or destroy.

;

UNCLASSIFIED

SECURITY CLASSIFICATION OF THIS PAGE (When Data Entered)

| REPORT DOCUMENTATION PAGE | | READ INSTRUCTIONS BEFORE COMPLETING FORM |
|--|-----------------------|--|
| 1. REPORT NUMBER RADC-TR-75-66 | 2. GOVT ACCESSION NO. | 3. RECIPIENT'S CATALOG NUMBER <i>AD-A008 521</i> |
| 4. TITLE (and Subtitle) REMOTE DETECTION OF THE HYDRONIUM ION | | 5. TYPE OF REPORT & PERIOD COVERED Final Technical Report 27 June 1973 - June 1974 |
| | | 6. PERFORMING ORG. REPORT NUMBER BEI-74-624 |
| 7. AUTHOR(s) Dr. Stanley M. Klainer | | 8. CONTRACT OR GRANT NUMBER(s) F30602-73-C-0360 |
| 9. PERFORMING ORGANIZATION NAME AND ADDRESS Block Engineering, Inc. Cambridge MA 02139 | | 10. PROGRAM ELEMENT, PROJECT, TASK AREA & WORK UNIT NUMBERS 61101F 01737308 |
| 11. CONTROLLING OFFICE NAME AND ADDRESS Rome Air Development Center (IRAD) Griffiss AFB NY 13441 | | 12. REPORT DATE March 1975 |
| | | 13. NUMBER OF PAGES 64 |
| 14. MONITORING AGENCY NAME & ADDRESS (if different from Controlling Office) Same | | 15. SECURITY CLASS. (of this report) UNCLASSIFIED |
| | | 15a. DECLASSIFICATION/DOWNGRADING SCHEDULE N/A |
| 16. DISTRIBUTION STATEMENT (of this Report) Approved for public release; distribution unlimited. | | |
| 17. DISTRIBUTION STATEMENT (of the abstract entered in Block 20, if different from Report) Same | | |
| 18. SUPPLEMENTARY NOTES RADC Project Engineer: Donald D. Dylis (IRAD) AC 315 330-7786 This effort was funded totally by the Laboratory Directors' Fund. | | |
| 19. KEY WORDS (Continue on reverse side if necessary and identify by block number) Raman Spectroscopy Aerosols Remote Detection Acid Concentration Hydronium Ion Hydrated Proton Acids | | |
| 20. ABSTRACT (Continue on reverse side if necessary and identify by block number) It was demonstrated that the hydronium ion can be remotely measured in acid solution and in acid aerosols. A Raman Spectrometric technique has been developed which indirectly measures aqueous acid concentrations. The approach is to measure the affect that acids and their salts have on the structure of the water solvent. Quantitative measurements of aqueous acid and salt solutions have been made for various concentrations. | | |

DD FORM 1473
1 JAN 73

EDITION OF 1 NOV 65 IS OBSOLETE

UNCLASSIFIED

1 SECURITY CLASSIFICATION OF THIS PAGE (When Data Entered)

Reproduced by
NATIONAL TECHNICAL
INFORMATION SERVICE
US Department of Commerce
Springfield, VA. 22151

SUMMARY

The program described in this report was designed to measure all the parameters necessary to establish that the hydronium ion can be measured in acid solutions and acid aerosols, and to assess the potential of remote measurement of atmospheric acidity using Raman Spectroscopy.

The results of this investigation have conclusively established that the Raman spectrometric technique gives quantitative information on acid concentrations. Data reduction methods have also been established, which permit identification of mono-nuclear anions when unknown or mixed acids are used.

TABLE OF CONTENTS

| | <u>Page</u> |
|---|-------------|
| Section I INTRODUCTION. | 9 |
| 1. General | 9 |
| 1.1 Purpose of Program. | 9 |
| 1.2 Program Results | 9 |
| 1.3 Program Background. | 9 |
| 1.4 The Raman Technique | 10 |
| 1.5 Program Plan. | 10 |
| II THEORETICAL DISCUSSION. | 13 |
| 2. Spectral Behavior of Materials of Interest. | 13 |
| 2.1 Bending Frequency Region. | 13 |
| 2.2 Stretching Frequency Region | 15 |
| 2.3 Component Analysis. | 17 |
| 2.4 Effects of Salts and Acids on H ₂ O Spectrum. | 18 |
| 2.5 Effect of Temperature | 18 |
| 2.6 Depolarization Measurements | 18 |
| 2.7 Solute and Solvent Effects. | 27 |
| 2.8 Frequency Shifts. | 30 |
| 2.9 Intensities of the High-Frequency Components. | 30 |
| 2.10 I ₃₂₂₀ /I ₃₄₂₅ Ratio | 32 |
| 2.11 Low Frequency Shoulder. | 33 |
| 2.12 Raman Intensities of Ion Pairs & Ionic Hydrates. | 33 |
| III EXPERIMENTAL MEASUREMENTS | 35 |
| 3. Spectral Characteristics of Materials of Interest | 35 |
| 3.1 Quantitative Analysis of Hydronium Ions in Aqueous Solutions. | 35 |
| 3.2 Experimental. | 35 |
| 3.3 Results and Discussion. | 38 |
| 3.4 Applications. | 38 |
| 3.5 Suggested Improvements. | 42 |
| IV ANALYSIS AND REVIEW | 45 |
| 4. Summarization of Probability of Detection Materials of Interest. | 45 |
| 4.1 Structure of the Hydrated Protons | 45 |
| 4.2 H ₃ O ⁺ : Hydronium Ion | 45 |
| 4.3 H ₅ O ₂ ⁺ : Bihydronium Ion or Biosonium Ion | 45 |
| 4.4 H ₇ O ₃ ⁺ | 47 |
| 4.5 H ₉ O ₄ ⁺ | 52 |

Preceding page blank

TABLE OF CONTENTS

| | | <u>Page</u> |
|------------|---|-------------|
| Section V | CONCLUSIONS. | 53 |
| 5. | General. | 53 |
| 5.1 | Results. | 53 |
| 5.2 | Direct Measurement of the Hydrated Proton | 53 |
| 5.3 | Acid Effects on the Structure of Water | 53 |
| 5.4 | Remote Detection | 54 |
| VI | RECOMMENDATIONS. | 55 |
| 6. | General. | 55 |
| 6.1 | Future Action. | 55 |
| 6.2 | Water Band Shape | 55 |
| 6.3 | Preliminary Field Tests. | 55 |
| 6.4 | Optimized Remote Raman Spectrometer. . . | 56 |
| APPENDIX A | RESEARCH LABORATORY RAMAN SPECTROMETER . . | 57 |
| 1. | Basic Raman Laboratory Spectrometer. . . | 57 |
| 1.1 | Instrument Calibration | 60 |
| 1.2 | Aerosol Cell | 60 |
| APPENDIX B | SENSITIVITY CALCULATIONS FOR THE REMOTE DETECTION OF AQUEOUS ACID CLOUDS | 61 |
| 1.0 | Remote Raman Parameters. | 61 |
| 1.01 | Remote Raman Spectrometer. | 61 |
| 1.02 | Atmospheric and Background Considerations | 61 |
| 1.03 | Aqueous Acid Clouds. | 62 |
| 1.04 | Operational Considerations | 62 |
| 1.1 | Pertinent Equations for Sensitivity Calculations | 62 |

TABLE OF FIGURES

| | <u>Page</u> |
|--|-------------|
| 1. Infrared Spectra of Water & HCl Solution | 14 |
| 2. Raman Spectra of H ₂ O and 6N HCl | 16 |
| 3. Isotropic Raman Spectrum of H ₂ O | 19 |
| 4. The Anisotropic Raman Spectrum of H ₂ O | 20 |
| 5. Anisotropic Raman Spectrum of H ₂ O showing Peaks | 21 |
| 6. Isotropic Raman Spectrum of 2N KCl | 22 |
| 7. Raman Spectrum of 2N HCl | 23 |
| 8. Raman Spectruun of 6N HCl | 24 |
| 9. Isotropic Raman Spectrum of 6N HBr | 25 |
| 10. Raman Spectra of H ₂ O, 3N KCl and 3N HCl | 26 |
| 11. Possible Structure of Water | 28 |
| 12. Schematic of an Ion | 28 |
| 13. Arrangement of Water Molecules | 31 |
| 14. Isotropic Raman Spectra of H ₂ O | 36 |
| 15. The Raman Spectrum of 2N HCl | 37 |
| 16. Specific Components of H ₂ O and HCl | 39 |
| 17. Relative Intensity vs. Concentration of Acid | 40 |
| 18. Intensity Ratio vs. Concentration of Acid | 41 |
| 19. Raman Spectrum of H ₂ O Aerosol | 43 |
| 20. Raman Spectrum of 6N HCl Aerosol | 44 |
| 21. Proposed Structure for H ₃ O ⁺ | 46 |
| 22. Proposed Structure for H ₅ O ₂ ⁺ | 48 |
| 23. Schematic Presentation of Vibrational Spectrum of H ₅ O ₂ ⁺ | 49 |
| 24. Proposed Structure for H ₇ O ₃ ⁺ | 50 |
| 25. Proposed Structures for H ₉ O ₄ ⁺ | 51 |
| 26. Block Diagram of Raman Spectrometer | 58 |
| 27. Block Diagram of Raman Spectrometer (with Dye Laser) | 59 |

EVALUATION

This investigation was conducted under the Laboratory Director's Fund Program to assess the potential of detecting, by remote means, the hydronium ion.

This effort demonstrated that the Raman spectrometric technique can be used to measure the hydronium ion in acid solutions and in acid aerosols, and that these measurements are directly related to quantification of acid content in the atmosphere.

Efforts in the area of Raman Spectroscopy, and its application to Air Force requirements will continue under the Exploratory Development Program, specifically under Project 5534, "Special Purpose Sensing Techniques" (TPO-2).



DONALD D. DYLLIS
Project Engineer

SECTION I

INTRODUCTION

1. GENERAL

1.1 Purpose of Program. The program described in this report was designed to measure all of the parameters necessary to determine if the hydronium ion can be measured in acid solutions and acid aerosols and to determine whether these measurements are directly related to quantification of the acid content. In addition, the potential of the remote measurement of atmospheric acidity using Raman spectroscopy was assessed. The program approached these measurements from both the theoretical and experimental aspects, with the major effort being experimental.

1.2 Program Results. The results of this investigation have established that the Raman spectrometric technique is ideally suited for the remote determination of acidity. It has been shown that this approach gives quantitative information on:

- (a) Aqueous acid aerosols
- (b) Aqueous acid solutions

In addition, data reduction methods have been established which permit mononuclear anions to be identified.

1.3 Program Background. In order to properly understand the extent of the acid problem, it is necessary to define "acidity." In general, an acid is defined as a proton-donor (1,2) or an electron-pair acceptor(3). In water solution, however, acid may be considered to be compounds capable of producing hydrogen ions, or better, hydronium ions (H_3O^+ or $H \cdot H_2O^+$). This is the situation which exists in acid solutions and in acid aerosols.

For remote measurement consideration, an atmospheric acid aerosol is defined as a gas/aqueous solution system being in equilibrium with each other. The aqueous phase contains

-
- (1) Bronsted, Rec. Trav. Chim., 42, 718 (1923).
 - (2) Lowry, Chem. and Ind., 42, 43 (1923).
 - (3) T. Moeller and R. O'Connor, "Ions in Aqueous Systems," McGraw-Hill Book Company (1972).

solvated acid compounds and has an "existing" acidity. The gaseous phase contains unsolvated acid compounds, and has a "potential" acidity. The total acid of this gas/aqueous solution system is defined as the total concentration of acid gases, acid-forming compounds, and acid solutions.

The specific problem addressed in this effort was to establish a technique to remotely measure "existing" acidity. The "potential" acidity can be measured by either Infrared or Raman spectroscopy techniques.

1.4 The Raman Technique. Raman spectroscopy is a proven technique for the remote detection, identification, and quantification of gases, liquids, aerosols, and solids. However, its ability to differentiate between water (H_2O) and the hydronium ion ($H\cdot H_2O^+$ or H_3O^+) in a liquid and/or aerosol had not been established. In addition, the existence of the hydronium ion in aqueous solutions had not been demonstrated. Both of these possibilities were investigated during this program.

1.5 Program Plan. The major tasks accomplished during this program were as follows:

(a) Calculate from Raman theory the location, bandwidth and intensity of the Raman spectral lines for H_3O^+ and other hydrates of the hydrogen ion. Calculate what parameters of the laboratory Raman instrument (such as resolution, irradiating wavelength, etc.) were required to see these lines in the presence of other species, such as water, which may be present.

(b) Verify, through laboratory experiments on a single acid (such as $HClO_4$), the validity of the theoretical calculations.

(c) Determine, through laboratory experiments, if other Raman lines exist for the hydrogen ion hydrates which were not anticipated from the theoretical calculations.

(d) Measure all of the characteristic parameters of the Raman lines from H_3O^+ and other hydrates for $HClO_4$. These included, but were not limited to Raman line shifts, Raman cross-sections, optimum excitation wavelengths, etc.

(e) Establish the exact relationship between measured values of H_3O^+ (and other hydrates) concentration, and acid concentration, in both solutions and aerosols.

(f) Repeat steps (d) and (e) for other acids such as HCl, HNO₃ and H₂SO₄.

(g) Predict, based on this work and on existing data on remote Raman system performance, the capabilities of remote detection of the hydronium ion and associated hydrates.

SECTION II

THEORETICAL DISCUSSION

2. SPECTRAL BEHAVIOR OF MATERIALS OF INTEREST

2.1 Bending Frequency Region. Figure 1 is the infrared spectra of varying concentrations of HCl (0, 3 and 6 N) in the region 2800-400 cm^{-1} . Very strong bands are observed in the spectrum of water at 1650, 690 and 2130 cm^{-1} . The 1650 cm^{-1} band, [which appears at a higher frequency compared to the vapor phase value (1591 cm^{-1}) (4)], has been assigned to the bending mode of the hydrogen-bonded water molecules.

Walrafen and Blatz (5) deconvoluted the vibrational contour of the 1650 cm^{-1} band using symmetric gaussian functions. Different components obtained thereby were explained in terms of the partially and fully hydrogen-bonded water molecules. Such a deconvolution may, however, be dubious because of the badly overlapping nature of the components. None of these are visually apparent from the spectra.

The position of the bending mode remains unaffected on addition of ions (see Figure 1 for HCl). Two additional bands are observed in acid solutions - one at 1730 cm^{-1} and the other at 1240 cm^{-1} . Intensities of these bands increase with the concentration of the hydrogen ions leading to visible separation of the 1730 cm^{-1} component at higher concentrations. The positions of these additional bands change very little on (a) increasing the concentration of hydrogen ions (1240 for 0.5 N HCl and 1230 for 6.0 N HCl) and (b) supercooling the solutions, thereby confirming the presence of specific entities in acidic solutions. By analogy with the absorptions of NH_3 (1650 and 1070 cm^{-1} in the condensed phase (6)), these additional bands at 1730 and 1240 cm^{-1} are assigned to the asymmetric ν_4 (E) and symmetric ν_2 (A) bending nodes of the pyramidal H_3O^+ respectively. Pyramidal

(4) G. Herzberg, Molecular Spectra and Molecular Structure, Vol. II, D. Van Nostrand Company, Inc., (1965).

(5) G. E. Walrafen and L. A. Blatz, J. Chem. Phys., 59, 2646, (1973).

(6) K. Nakamamoto, Infrared Spectra of Inorganic and Coordination Compounds, John Wiley and Sons, (1963).

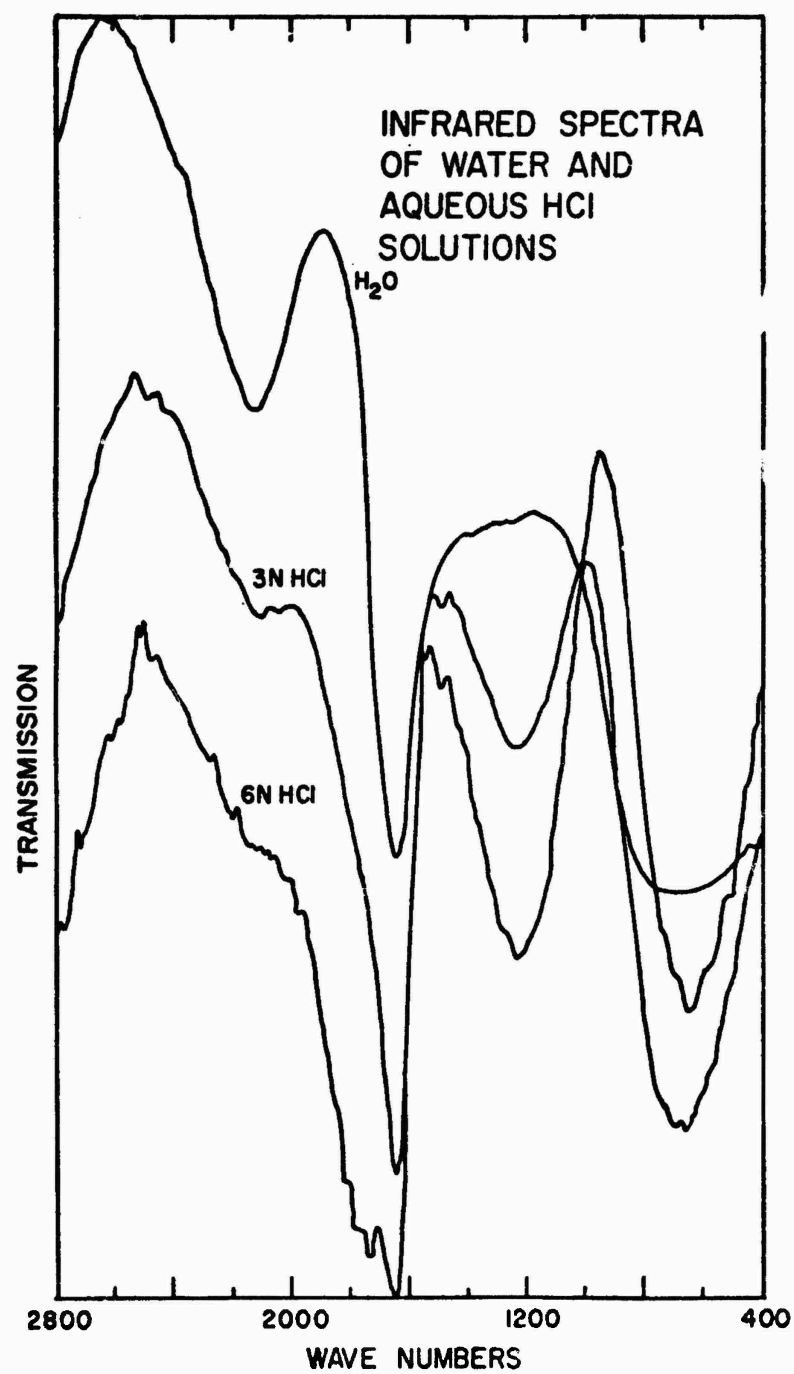


Figure 1. Infrared Spectra of Water and HCL Solutions.

structure for H_2O^+ is supported by X-ray^(7,8,9), nuclear magnetic resonance^(10,11) and infrared⁽¹²⁾ work in the solid state and is tentatively regarded so in the solution.

Both additional bands are allowed in the Raman and are, moreover, observed in the solid state. They, however, disappear in solution (see Figure 2). This may be explained on the basis of the concept of polarizability and the dilution of the crystalline forces in solution.

The other two bands observed around 690 cm^{-1} and 2130 cm^{-1} , which are present in all the aqueous solutions have been assigned to the vibrational (ν_{L_3}) and the combinations ($\nu_{\text{L}_1} + \nu_2$) of the H_2O bands. The position of these bands is also unaffected.

Intensity of the ν_2 Raman band of H_2O increases manyfold on addition of ionic solutes. The increase is approximately linear and decreases in order $\text{I}^- > \text{Br}^- > \text{Cl}^- > \text{F}^-$. There is very little cationic effect. Another noticeable change in the Raman spectra (Figure 2) is the decrease in the half-width of the bending mode. The rather large intensity variations for the more polarizable anions indicate considerable covalent character in the water-anion interactions and it is surprising that there is no corresponding change in the band position.

2.2 Stretching Frequency Region. The OH stretching region of water, which extends from $2700\text{--}3800\text{ cm}^{-1}$ appears very confused

(7) J. O. Lundgren and J. M. Williams, J. Chem. Phys., 58, 788, (1973).

(8) J. O. Lundgren, Acta Cryst., 28B, 475, (1972).

(9) R. Savoie and P. A. Giguere, J. Chem. Phys., 41, 2698, (1964).

(10) R. E. Richards and J. A. S. Smith, Trans. Faraday Soc., 48, 1216, (1951).

(11) Y. Kakiuchi et al, J. Chem. Phys. 19, 1069, (1951).

(12) J. O. Lundgren and J. M. Williams, J. Chem. Phys., 58, 788, (1973).

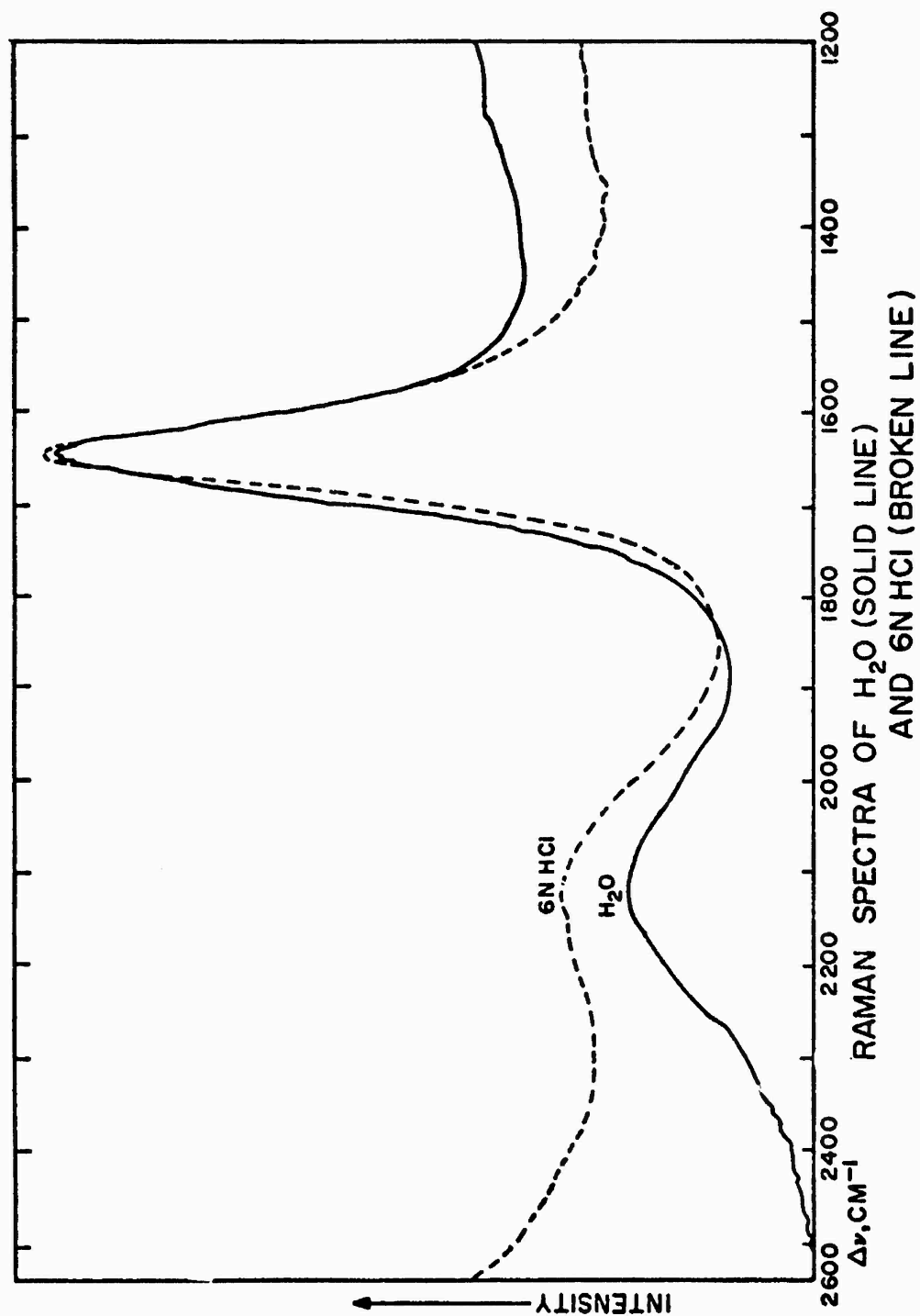


Figure 2. Raman Spectra of H_2O and 6NHCL .

and has been the subject of a number of recent studies (13,14,15). Absorptions due to H_3O^+ lead to a trailing lower frequency shoulder. This further complicates the band extending it to the 2500 cm^{-1} region.

2.3 Component Analysis. The Raman spectra of H_2O and D_2O provide visual evidence for the presence of three components around 3615 , 3425 and 3250 cm^{-1} for H_2O and 2660 , 2500 and 2380 cm^{-1} for D_2O . Deconvolution of this band into Gaussian and Lorentz type components has been attempted by many workers. The two functions are very similar above half height but the base of the Lorentz function is much broader and it has extended wings. Schultz and Hornig (16) obtained a reasonable fit using three gaussian functions. When the bands were fitted to Lorentz functions, the calculation did not converge and a unique solution could thus not be obtained.

With the use of pure gaussian functions, Walrafen (13) deconvoluted the photoelectronically recorded contour into four curves. There are five components in H_2O , the fifth being very weak as shown in Figure 4. Murphy and Bernstein (14) used symmetric Gaussian-Lorentz product functions of the type

$$I(\nu) = \frac{x_1 \exp [-x_4 (\nu-x_2)^2]}{1 + x_3 (\nu-x_2)^2} \quad (3-1)$$

where the parameters x_1 , x_3 and x_4 were varied to obtain the best fit in the least-squares sense. The band position was constrained to be equal for the isotropic and anisotropic components of a single band. Four functions, consistent with their proposed model, were used for fitting the contours of the isotropic spectra; a fifth band was, however, found necessary for the anisotropic spectra. The decomposition into four components is supported by the mutually exclusive stimulation of the two low frequency components in water and the other two high frequency components in sodium perchlorate solutions. Further evidence is provided by the visual separation of the fourth

(13) F. Franks, editor, The Physics and Physical Chemistry of Water, Vol. I, Plenum Press, (1972).

(14) W. F. Murphy and H. J. Bernstein, J. Phys. Chem. **76**, 1147, (1972).

(15) G. E. Walrafen, J. Solution Chem., **2**, 159, (1973).

(16) J. W. Schultz and D. F. Hornig, J. Phys. Chem., **65**, 2131, (1961).

component (a) in aqueous solutions of NaClO_4 and (b) at high temperatures.

In the present work (Figures 3 to 9), symmetric gaussian functions have been employed. Both position and half-width of a single component were maintained constant for all the recorded spectra. Raw data were used directly for band-fittings. The frequencies reported here have an estimated error of 0 to $\pm 20 \text{ cm}^{-1}$.

2.4 Effects of Salts and Acids on H_2O Spectrum. The total integrated intensity of the OH stretch is found to increase with the addition of the ionic solutes. The increase is, however, much smaller than that observed for the bending mode. Shown in Figure 10 are the smoothed Raman spectra of H_2O , 3 N HCl and 3 N KCl. These spectra were recorded with different laser outputs and different count rates and, therefore, should not be compared for absolute intensities. Comparisons of the overall vibrational contours, however, indicate a remarkable change in the relative intensities of the two strong components on addition of ionic solutes. Other noticeable changes are: (a) a significant decrease in the high frequency component compared to that of the strongest band; (b) a slight increase in the frequency of the maximum and (c) an additional trailing band in the acid solutions. All these changes increase with the concentration of the added solute. Fluorides are found to have opposite and a smaller effect. Variations in the half-widths could not be studied because of the changes in the relative frequencies of the components concerned. Weston (17), from his studies on the Raman spectra of OH and OD bands in HDO, indicated that the bands become narrower in electrolytic solutions of various alkali halides except KF. The band width was also found to be dependent on the concentration of the ions.

2.5 Effect of Temperature. The effects of temperature between the range $2-95^\circ \text{C}$ has been studied by Schultz and Hornig (16). The changes were similar to those observed on addition of salts except that the highest frequency component was found to increase relative to the strongest band.

2.6 Depolarization Measurements. Depolarization ratios of H_2O and D_2O change across the band indicating the presence of more than one component. The value of ρ increases with frequency but is always below the value of $6/7$ required for an antisymmetric vibration. Recorded values for the components of H_2O (as shown in Table 1) agree well with those reported by Murphy and

(17) R. E. Weston, Jr., *Spectrochimica Acta*, 18, 1257, (1972).

ISOTROPIC RAMAN SPECTRUM
OF H_2O AND ITS COMPONENTS
(HALF BAND-WIDTHS AND PEAK
HEIGHTS ARE SHOWN BY STRAIGHT
LINES).

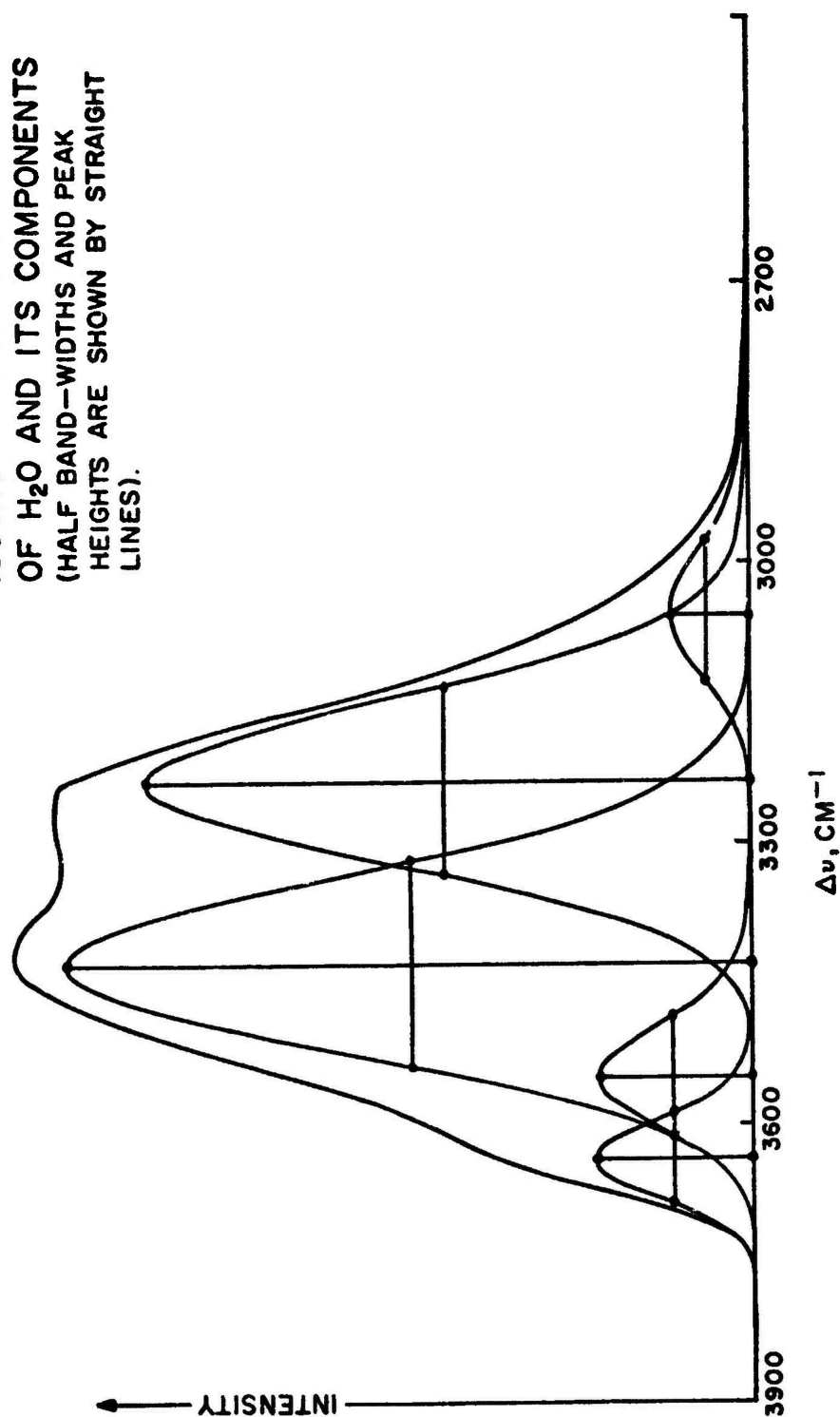


Figure 3. Isotropic Raman Spectrum of H_2O .

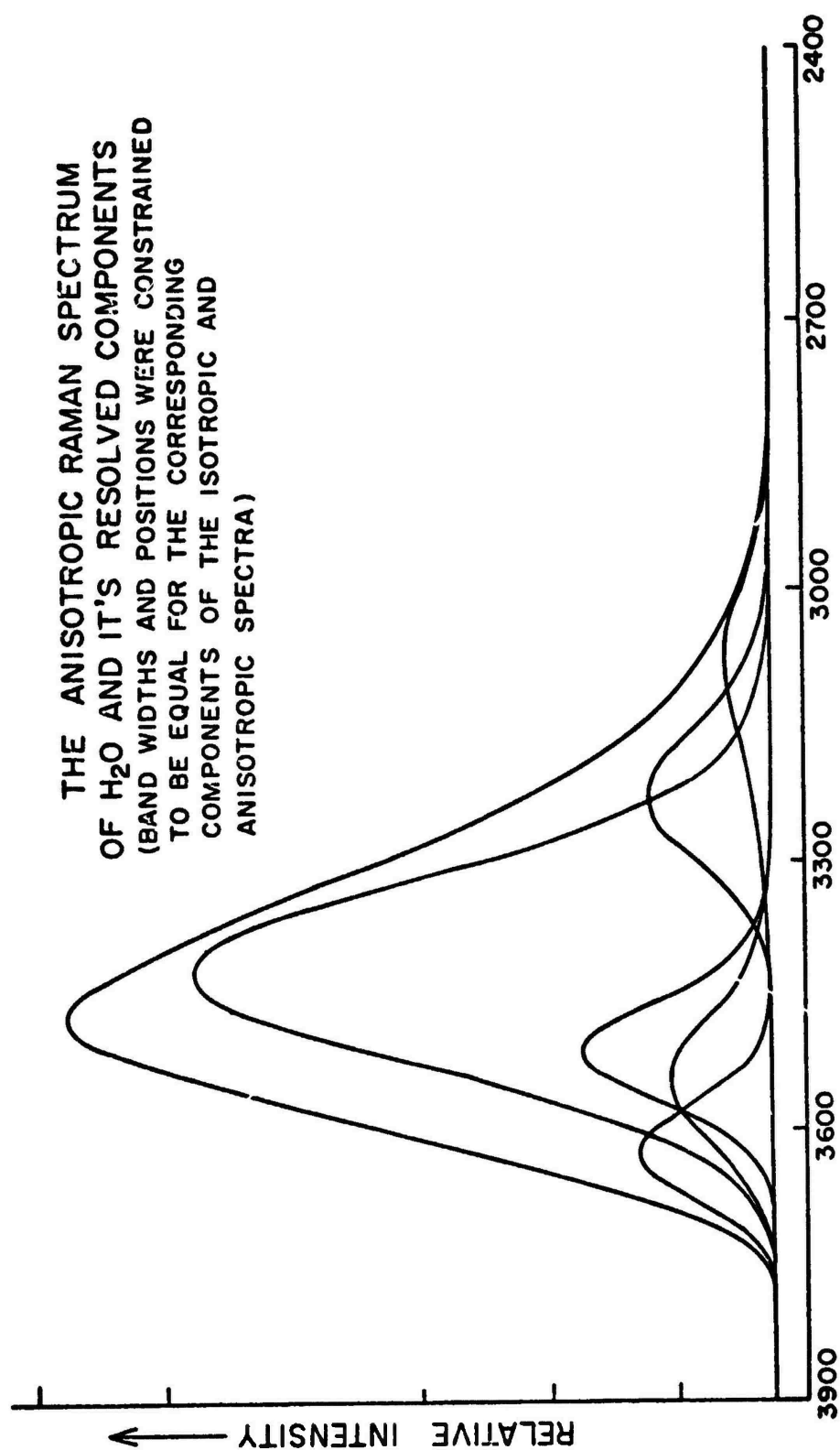


Figure 4. The Anisotropic Raman Spectrum of H₂O.

ANISOTROPIC RAMAN SPECTRUM OF
H₂O AND ITS RESOLVED COMPONENTS

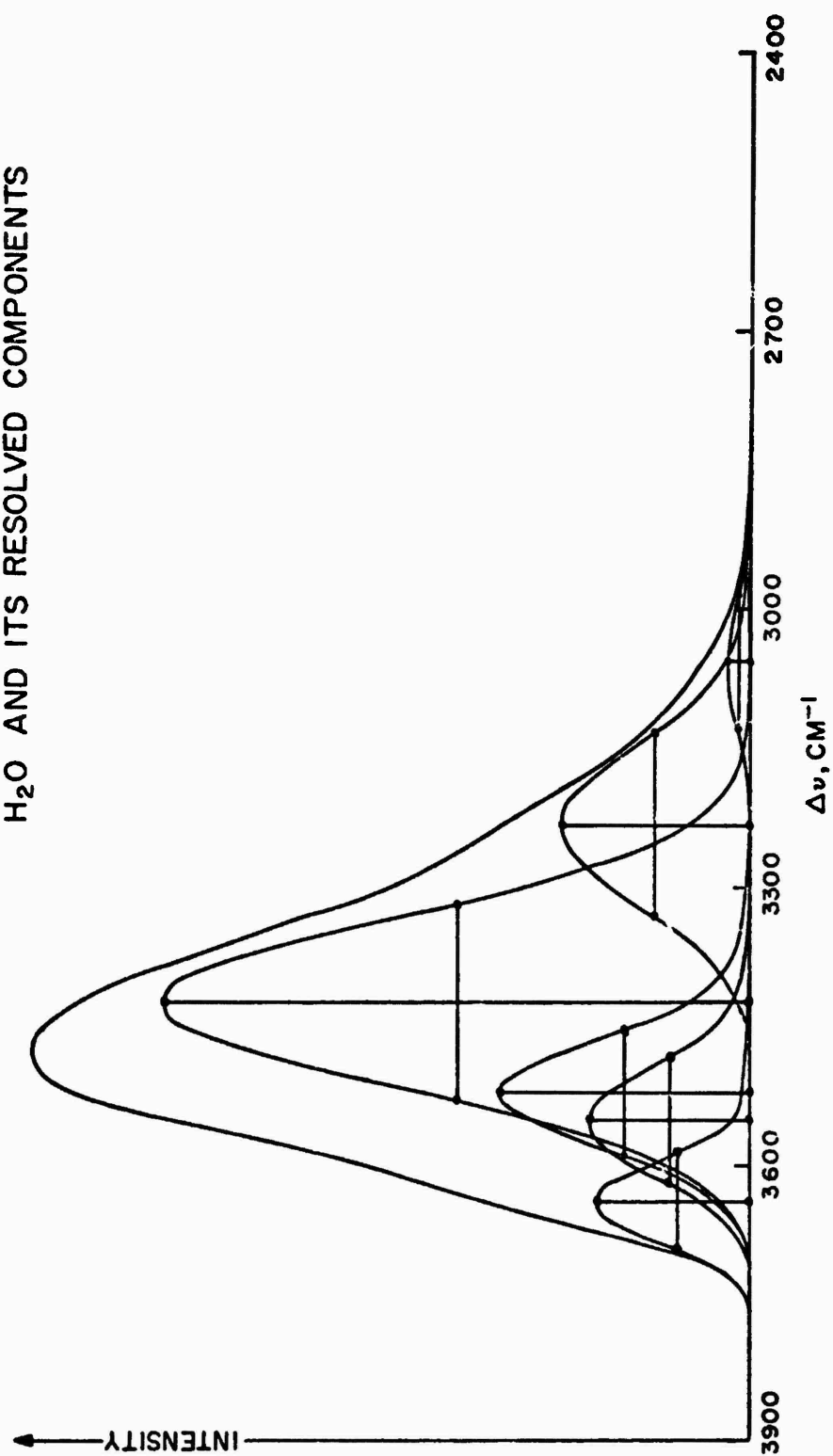


Figure 5. Anisotropic Raman Spectrum of H₂O Showing Peaks.

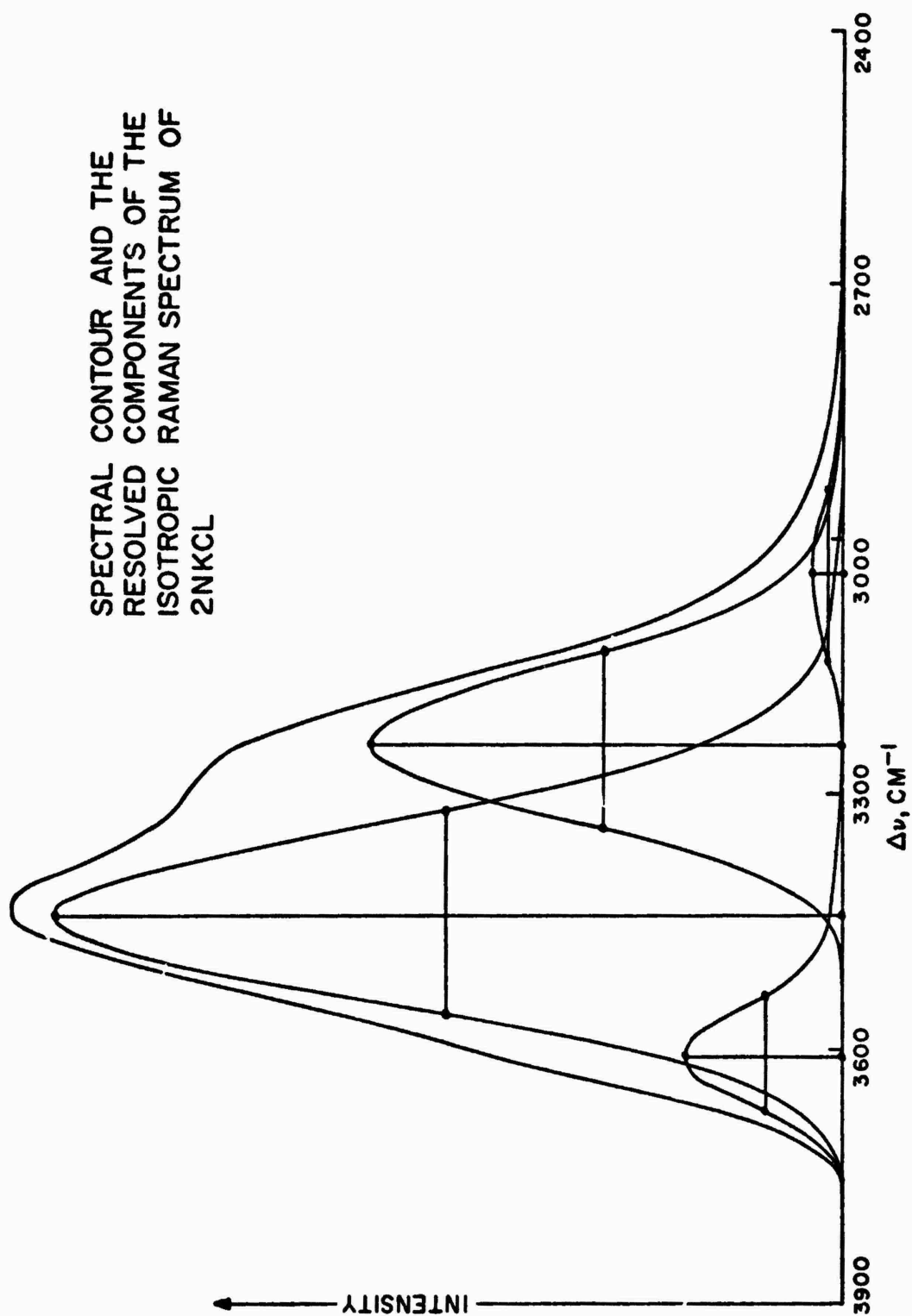


Figure 6. Isotropic Raman Spectrum of 2NKCl.

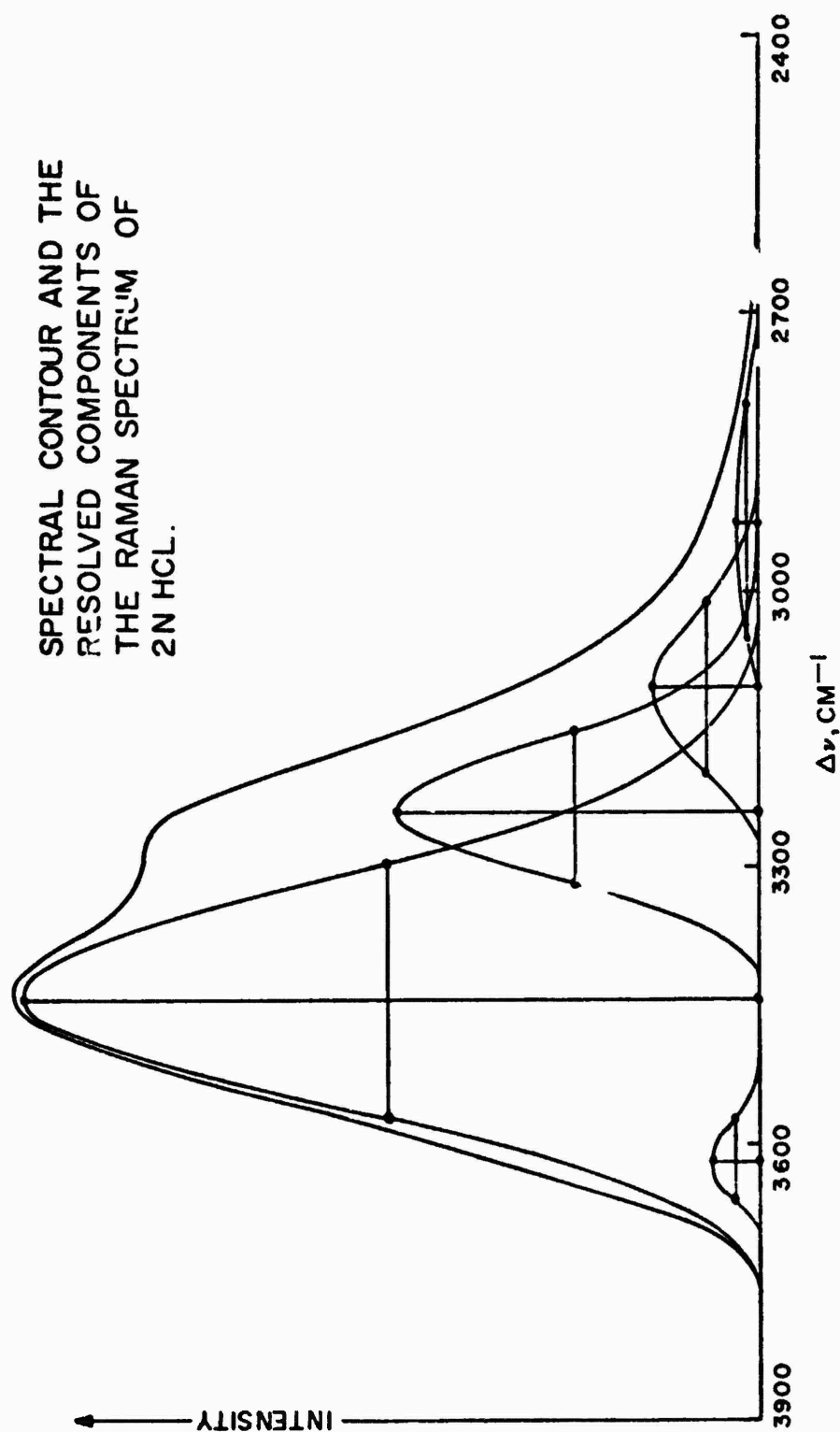


Figure 7. Raman Spectrum of 2NHCl.

ISOTROPIC RAMAN SPECTRUM OF
6N HCl AND ITS DECONVOLUTED COMPONENTS

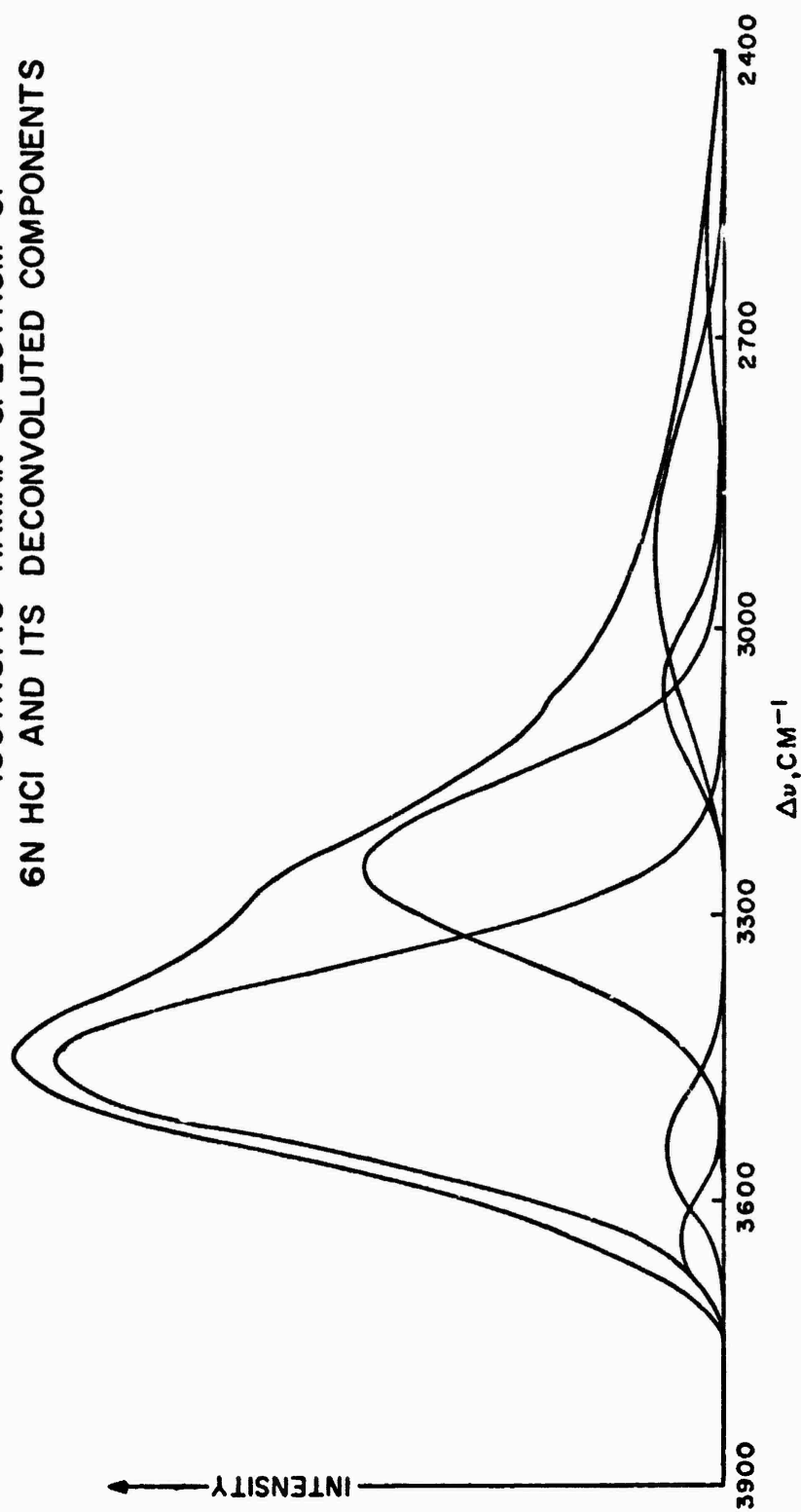


Figure 8. Raman Spectrum of 6N HCl.

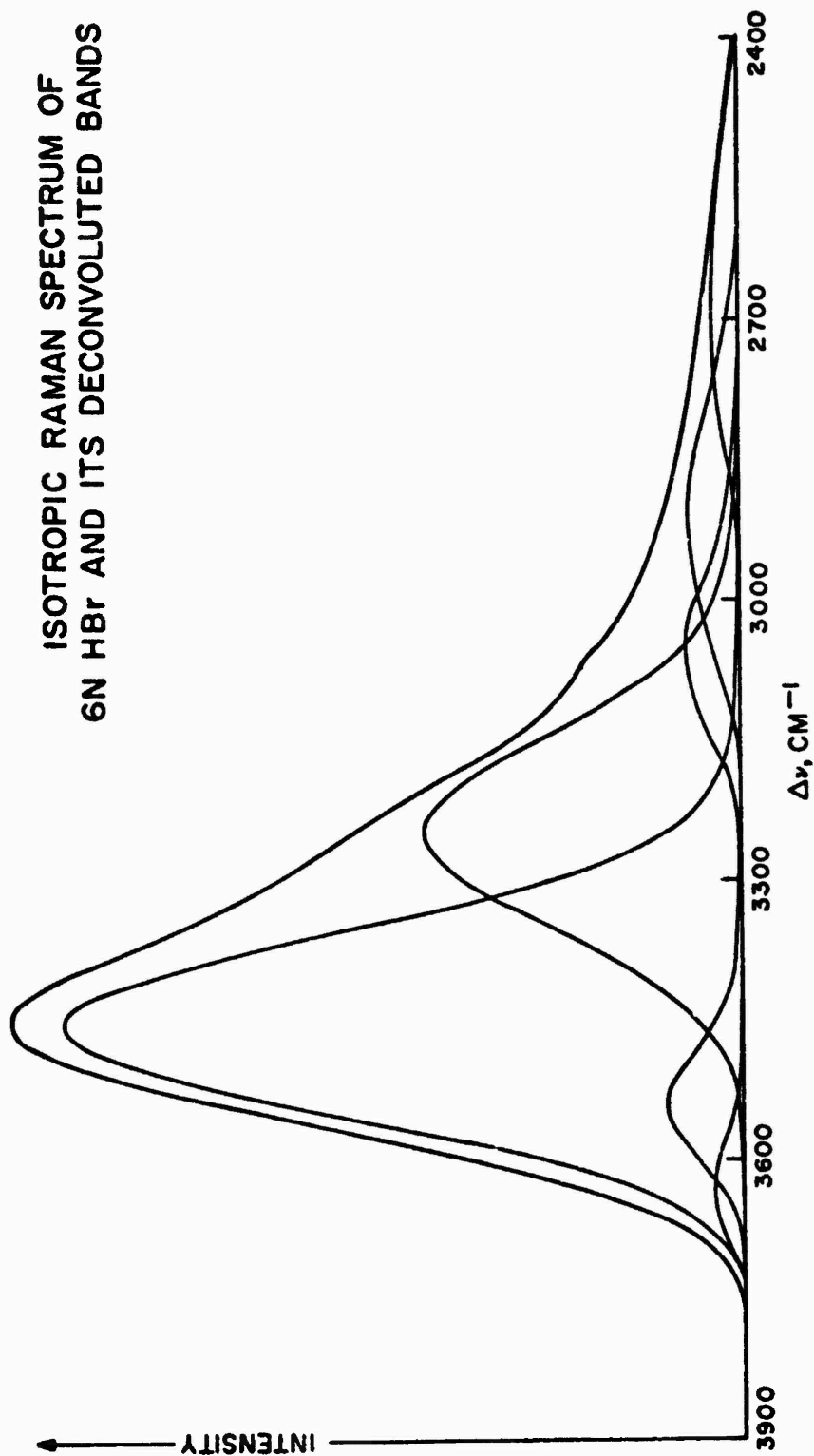


Figure 9. Isotropic Raman Spectrum of 6N HBr.

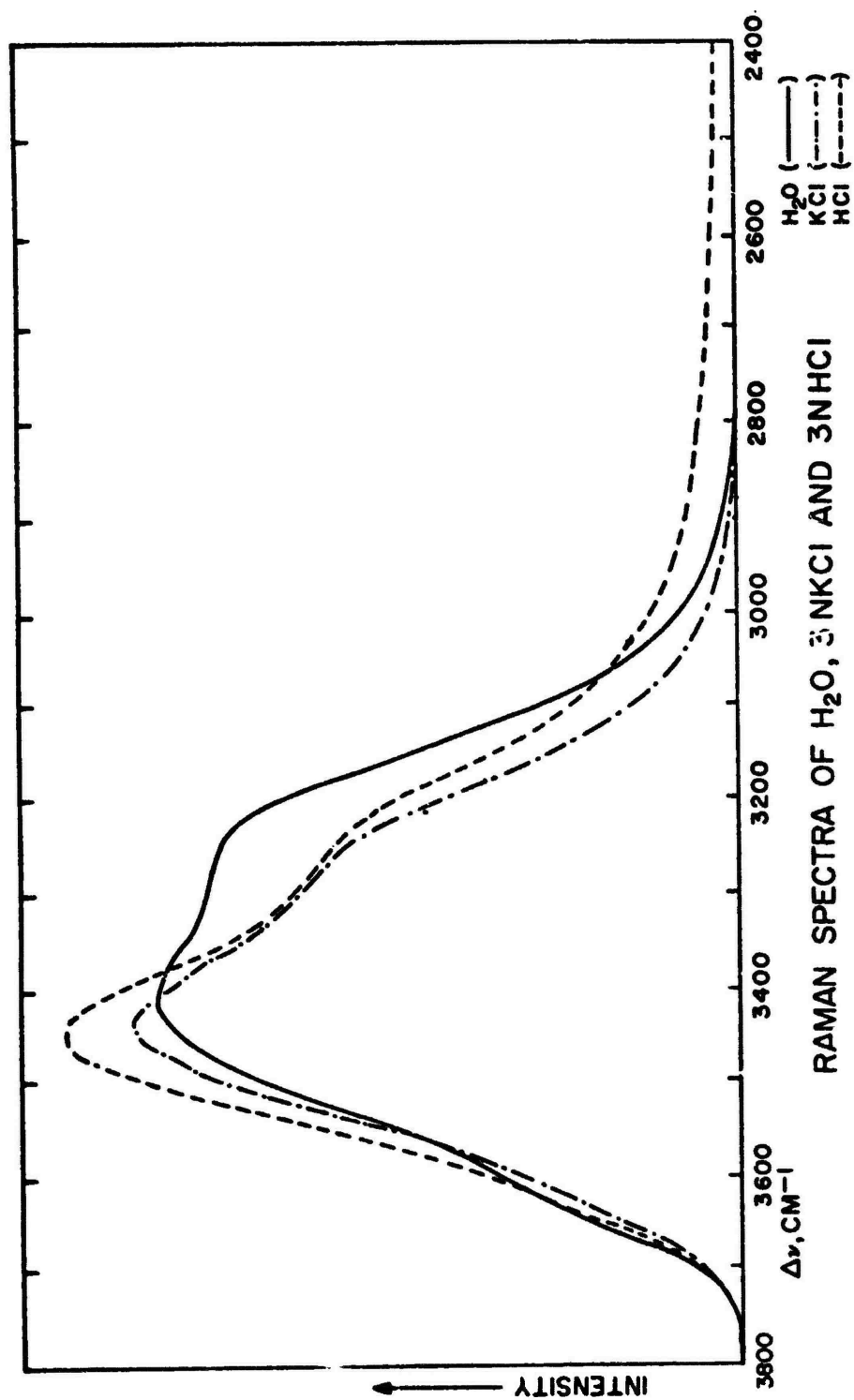


Figure 10. Raman Spectra of H_2O , 3N KCl and 3N HCl.

Bernstein. Also listed in Table 1 are the values for different solutions. Comparisons in Table 1 indicate that the depolarization ratio stays relatively constant for the 3450 cm^{-1} band whereas those of 3225 cm^{-1} and 3080 cm^{-1} bands increase with the concentration of the added solute. The values reported for the low frequency components of acidic solutions should be regarded as arbitrary because of the reasons discussed later.

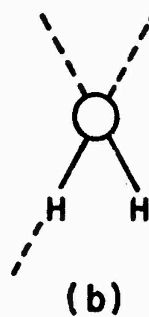
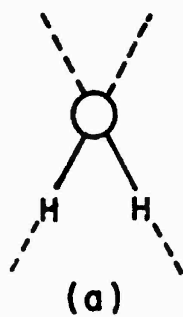
TABLE I
DEPOLARIZATION MEASUREMENTS*

| H_2O | | 2N KCl | | 2N HCl | | 2N HBr | | 6N HCl | | 6N HBr | |
|----------------------|--------|--------|--------|--------|--------|--------|--------|--------|--------|--------|--------|
| ν | ρ | ν | ρ | ν | ρ | ν | ρ | ν | ρ | ν | ρ |
| 3630 | .18 | 3630 | .27 | 3635 | .24 | 3635 | .25 | | | | |
| 3550 | .26 | 3550 | .28 | 3555 | .34 | 3555 | .23 | | | | |
| 3415 | .17 | 3425 | .17 | 3425 | .19 | 3430 | .18 | 3440 | .22 | 3440 | .2 |
| 3220 | .05 | 3230 | .06 | 3230 | .07 | 3235 | .07 | 3235 | .17 | 3235 | .17 |
| 3075 | .07 | 3080 | .09 | 3080 | .09 | 3080 | .09 | 3090 | .19 | 3090 | .16 |
| | | | | 2850 | .09 | 2830 | .06 | 2925 | .2 | 2925 | .16 |
| | | | | | | | | 2725 | .17 | 2725 | .16 |
| 3520 | .75 | 3490 | .75 | 3490 | .75 | 3490 | .75 | 3400 | .75 | 3415 | .75 |

*The position and width of the bands were constrained to be equal for the isotropic and anisotropic components of a single band.

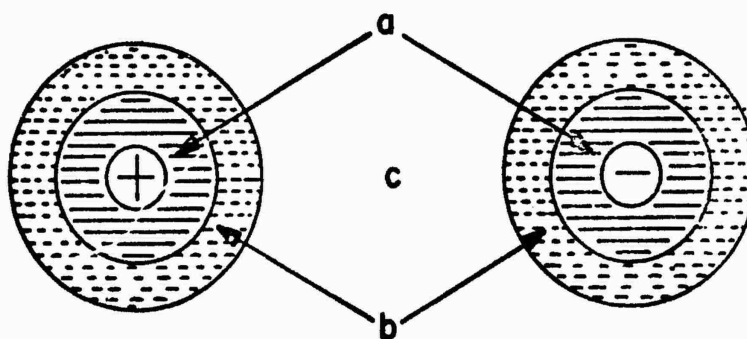
2.7 Solute and Solvent Effects. Knowledge of the structure of liquid water is obviously the first step towards understanding the nature of ion-liquid interactions. Various models have been proposed to account for the properties of liquid water. Vibrational spectra have often been used to support these models which in turn provide explanations for the various observed features. Two different models, which have been proposed to account for the spectral features of H_2O , will be used to explain the vibrational features observed in aqueous solutions. One of these is due to Murphy and Bernstein⁽¹⁴⁾ and the other one is due mainly to Walrafen⁽¹³⁾.

According to Murphy and Bernstein, the four component structure of water arises from two types of molecules (Figure 11) viz: tetracoordinated (type a) and tricoordinated having a free hydrogen (type b). Furthermore, because of the predominance of the fully hydrogen-bonded species over the tricoordinated, the intense bands are due to the former and the weaker



POSSIBLE STRUCTURE OF WATER

Figure 11. Possible Structure of Water.



SCHEMATIC OF AN ION IN DILUTE AQUEOUS SOLUTION

Figure 12. Schematic of an Ion.

ones due to the latter. The two higher frequency components at 3620 cm^{-1} and 3565 cm^{-1} were thus assigned to the non hydrogen-bonded components of (b). The remaining two strong features at 3420 cm^{-1} and 3225 cm^{-1} have been ascribed to Fermi resonance of the symmetric component of (a) with the first overtone of its bending mode. The additional component in the anisotropic spectrum was assigned to the asymmetric component ν_3 of (a).

Walrafen, on the other hand, has described the OH vibrational contour on the basis of fully and non hydrogen-bonded molecules. The high frequency side which is closer to the monomeric OH stretch (3655 cm^{-1}) and the intensity of which increases with temperature has been ascribed to the non hydrogen-bonded species. Two components in each major class are regarded as due to vibrational coupling within molecules of each major class leading to in-phase and out-of-phase components. Thus 3420 cm^{-1} and 3225 cm^{-1} bands are due to the two components of the hydrogen-bonded molecules whereas 3620 cm^{-1} and 3565 cm^{-1} curves are due to the non hydrogen-bonded species. The fifth component at 3080 cm^{-1} may arise from Fermi resonance between the component at 3225 cm^{-1} with the first overtone of the bending mode.

Both models discussed favor a discontinuum model for the structure of liquid water and one may refer to the original articles for their relative advantages and shortcomings. In fact none of the above models explains all the observed spectral features and are neither totally consistent with the other physical properties of the system. Complexity of the system increases on addition of ionic solutes. The added material not only adds to existing interactions but also perturbs the original solvent-solvent interactions. Much experimental data exists on such systems and many theories have been put forward to explain the observed facts. Out of these, a simple theory proposed by Frank and Wen⁽¹⁸⁾ seems to provide a rationale to most of the observed spectral features and will be used to explain the observed behavior.

According to Frank and Wen⁽¹⁸⁾, an ion in a dilute aqueous solution may be regarded as surrounded by three different regions, (a) an innermost structure forming region of polarized, immobilized and electrostricted water molecules, (b) an intermediate structure-breaking region in which the water is less ice-like and (c) an outer region containing water having the normal liquid structure. See Figure 12. Relatively small and multivalent ions such as Li^+ , Na^+ , H_2O^+ , Ca^{2+} , Ba^{2+} , Mg^{2+} , OH^- ,

(18) H. S. Frank and W. Y. Wen, Disc. of the Faraday Soc., 24, 133, (1957).

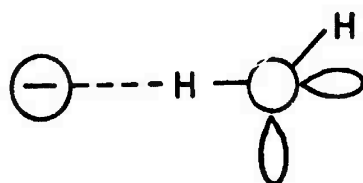
F^- increase the viscosity of water and are said to have net structure making effects whereas large monovalent ions such as K^+ , NH_4^+ , Rb^+ , Cs^+ , Cl^- , Br^- , I^- , NO_3^- , BrO_3^- , IO_3^- , ClO_4^- increase the fluidity of water and have thus a net structure breaking effect (entropy increases). As the concentration of the solute is increased, the oppositely charged ions approach more closely and the solute-solute forces become more important than those due to the solute-solvent interaction. Of course, interactions from like charged species and contributions from higher aggregates of ionic species also become significant. In concentrated solutions, therefore, the situation becomes rather more complicated and in view of this the discussion that follows will be limited only to dilute solutions.

2.8 Frequency Shifts. The frequency shifts observed on addition of ionic solutes may be explained in terms of solute-water interactions. The net structure makes the ions polarize, immobilize and electrostrict the nearest neighbor water molecules, inducing additional order beyond the first layer. This should lead to a decrease in the frequency of ν_1 . Net structure breaking ions can cause polarization, immobilization and electrostriction only in the first layer leaving the central region free of the electrostatic fields, and thus there is an increase in the frequency of ν_1 . Observed frequency shifts due to anions correlate well with expectations based on structural effects and are also consistent with other physical properties. Cations which are also expected to exhibit similar behavior, however, do not show significant frequency shifts, and the shift obtained from LiCl and CsCl are about the same. Intuitively, it may be concluded that this may be due to the difference in the arrangements of the water molecules around the ions, as shown in Figure 13. Water molecules in the primary hydration shell of the cation would thus have the H atoms away from the ion, whereas water molecules adjacent to the anion would have the hydrogen atoms directed towards the ion. If the interaction between the ion and water is predominantly electrostatic in nature then the effect would not be transmitted to the O-H bond of the cation to any significant extent. Increase in temperature increases the disorderness thereby increasing the frequency.

2.9 Intensities of the High-Frequency Components. Both cations and anions may be expected to decrease the intensities of the non hydrogen-bonded (high-frequency) components primarily because of the water molecules needed for the immediate hydration sphere. Current experimental findings are consistent with these expectations and also explain why Schultz and Hornig⁽¹⁶⁾ could not observe the high frequency components in a concentrated solution of LiI (7.9 M). An increase in the temperature on the other hand, would be expected to increase the concentration of the non hydrogen-bonded species. Aqueous solutions of ClO_4^- and IO_4^- are found to have spectra similar to those of the solvent at high temperatures. Thus it appears that the aqueous solutions of



(a.) AROUND A CATION



(b.) AROUND AN ANION

Figure 13. Arrangement of Water Molecules.

ClO_4^- and IO_4^- behave like high temperature water systems. It may, therefore, be concluded that perchlorate ions do not associate themselves with any significant number of free water molecules so as to decrease their concentration. Consequently, the intensities of the higher frequency components can be used for determining the hydration number of the anions. A rigorous analysis can shed some light on the different models used for explaining the vibrational contour of water.

2.10 I_{3220}/I_{3425} Ratio. The ratio of the intensities of the two strong bands and its variation in ionic solutions may be explained on the basis of the concept of Fermi resonance. The perturbed frequencies of the Fermi doublet are related to the unperturbed frequencies ν_1^0 and $2\nu_2^0$ by

$$\nu_1 + 2\nu_2 = \nu_1^0 + 2\nu_2^0 \quad (3-2)$$

For harmonic oscillations, the ratio of the intensities of the two bands is given by

$$\frac{I_{2\nu_2}}{I_{\nu_1}} = \frac{\Delta - \delta}{\Delta + \delta} \quad (3-3)$$

where

$$\Delta = \nu_1 - 2\nu_2$$

and

$$\delta = \nu_1^0 - 2\nu_2^0.$$

From the resolved components of the band Δ is 195 cm^{-1} whereas the sum of ν_1 and $2\nu_2$ is 6635. Without the knowledge of anharmonicity one cannot calculate $2\nu_2^0$ from the observed fundamental frequency (1650 cm^{-1}) but an upper limit of its value is given by twice the value of the fundamental, i.e. 3300 cm^{-1} . This gives an upper limit of 0.7 for the intensity ratio. The calculated value is in the range of the values (0.6 to 0.9) determined experimentally. Large range of the experimental values is due to the dependence of the ratio on the relative positions and shapes of the bands concerned.

If there is no interaction, the intensity of the overtone band would have been very low. The enhancement of the intensity is thus a result of this interaction. Fermi interaction, which arises between two levels of the same symmetry, is a function of the distance between the interacting levels. From the results described earlier, it appears that ν_2^0 (and hence $2\nu_2^0$) is unaffected in solutions whereas ν_1^0 is changed. A decrease in the value of ν_1 will then increase the amount of interaction thereby resulting in the enhancement of the overtone band; an increase will have the opposite effect. Increase in temperature and the addition of structure breaking anions would thus decrease the

ratio whereas the structure forming anions would tend to raise it. Cations on the other hand should leave the ratio unchanged, as they do not change the separation of the two interacting levels. The observed spectral features are in agreement with the expectations based on this hypothesis. A quantitative judgement, however, requires an accurate knowledge of the frequency shifts and relative intensities.

Variations in the ratio can also be explained in terms of the intermolecular coupling between each major class. Lack of the understanding of the intermolecular forces, however, does not affect the ability to perform quantitative analysis provided proper calibration had been performed. It would thus appear premature to ascribe this ratio to any particular effect until a more quantitative analysis is carried out.

2.11 Low Frequency Shoulder. Growth in the intensity of the low frequency shoulder with the increase in the concentration of the acid indicates the formation of new species. At low concentrations, the trailing end can be described by a broad Gaussian component centered around 2925 cm^{-1} . Two such components at 2925 and 2725 cm^{-1} are, however, needed to match the vibrational contour at very high concentrations.

If these components were due mainly to H_3O^+ , one would have expected depolarization ratios corresponding to that of equal symmetric and antisymmetric stretching vibrations. The observed depolarization ratios, however, do not permit unambiguous assignment of these components to symmetric and antisymmetric modes. Evidence exists that protons in solution bind to varying number of water molecules. If this is so, and the different species have Raman active transitions, then the decomposition of the contour into two components may be an artifact. Theoretical calculations indicate that H_3O^+ has a small barrier to inversion. This kind of a motion, though very inhibited in solution, can also alter the shape of the bands. The observed ratio in this region should, therefore, be regarded as tentative and the resolved components may be regarded as due to hydrated protons (H_3O^+) provided that the uncertainty which still exists is fully realized.

2.12 Raman Intensities of Ion Pairs and Ionic Hydrates. One of the obvious limitations of this investigation is that only those solutes can be studied which have Raman-allowed transitions. Intensities of these bands depend, furthermore, upon the change in the polarizability accompanying that particular mode. The absence of stretching vibrations between anions and cations linked by pure electrostatic bonds, therefore, implies that the molecular polarizability in such cases is independent of the interionic distances.

In solutions, ions may exist as direct ion pairs or as solvent separated ion pairs (held together by electrosolvent molecules). An ion-dipole interaction is clearly an adequate description of the bonding between water molecules and simple ions, therefore, some degree of covalence is expected. Raman lines corresponding to ion-water bonds have in fact been characterized in a few molecules except those of first and seventh group ions. A clear distinction between direct ion-pairs and solvent separated ion pairs is, however, very difficult because of the weak nature of the bonds.

SECTION III

EXPERIMENTAL MEASUREMENTS

3. SPECTRAL CHARACTERISTICS OF MATERIALS OF INTEREST

3.1 Quantitative Analysis of Hydronium Ions in Aqueous Solutions

The usefulness of Raman spectroscopy in quantitative measurements of molecular species is well established. The method, invariably, consists of following the concentration dependence of a well separated Raman band. A possible complication in the investigation of Raman active species in solution arises in that the selection rules for transitions may be less rigorously obeyed than they would be in situations where the molecular species is more easily defined. This means that only those solutions containing polyatomic ionic species are amenable to direct study, and the theoretically more important and simplest ionic solutions, namely those containing monoatomic ions, are precluded from such investigations.

Detailed investigations of these solutions, employing deconvolution procedures, however, indicate that changes in the spectral concentrations, should provide reliable procedures for quantifying monoatomic ions in solution. Varying concentrations of HCl, KCl, and H₂SO₄ (preliminary) have been used to demonstrate the feasibility of such studies.

3.2 Experimental

Raman spectra were recorded for several concentrations of HCl, KCl and H₂SO₄ in the range 2400-3900 cm⁻¹. Instrumental parameters were maintained constant for different concentrations of the same compound. Straight lines, drawn across the base of the bands, were assumed as the true base lines. This was necessary only in concentrated acid solutions.

Spectral contour of water was deconvoluted, with a duPont Model 310 curve resolver, using symmetric gaussian functions centered exactly at 3635, 3415, 3225, and 3060 cm⁻¹, as shown in Figure 14. An additional component located at 2925 cm⁻¹ (Figure 15) was employed for acid solutions. Band positions and widths were constrained to be equal for all the remaining spectra, and the data were fitted by varying just the peak-heights. An excellent fit to the data indicated consistency of the procedure.

Areas of the component bands, relative to one of the intense bands, were read directly from an integrator attached directly to the curve resolver. These measurements involve an error of about $\pm 1\%$.

ISOTROPIC RAMAN SPECTRUM
OF H_2O AND ITS COMPONENTS
(HALF BAND-WIDTHS AND PEAK
HEIGHTS ARE SHOWN BY STRAIGHT
LINES).

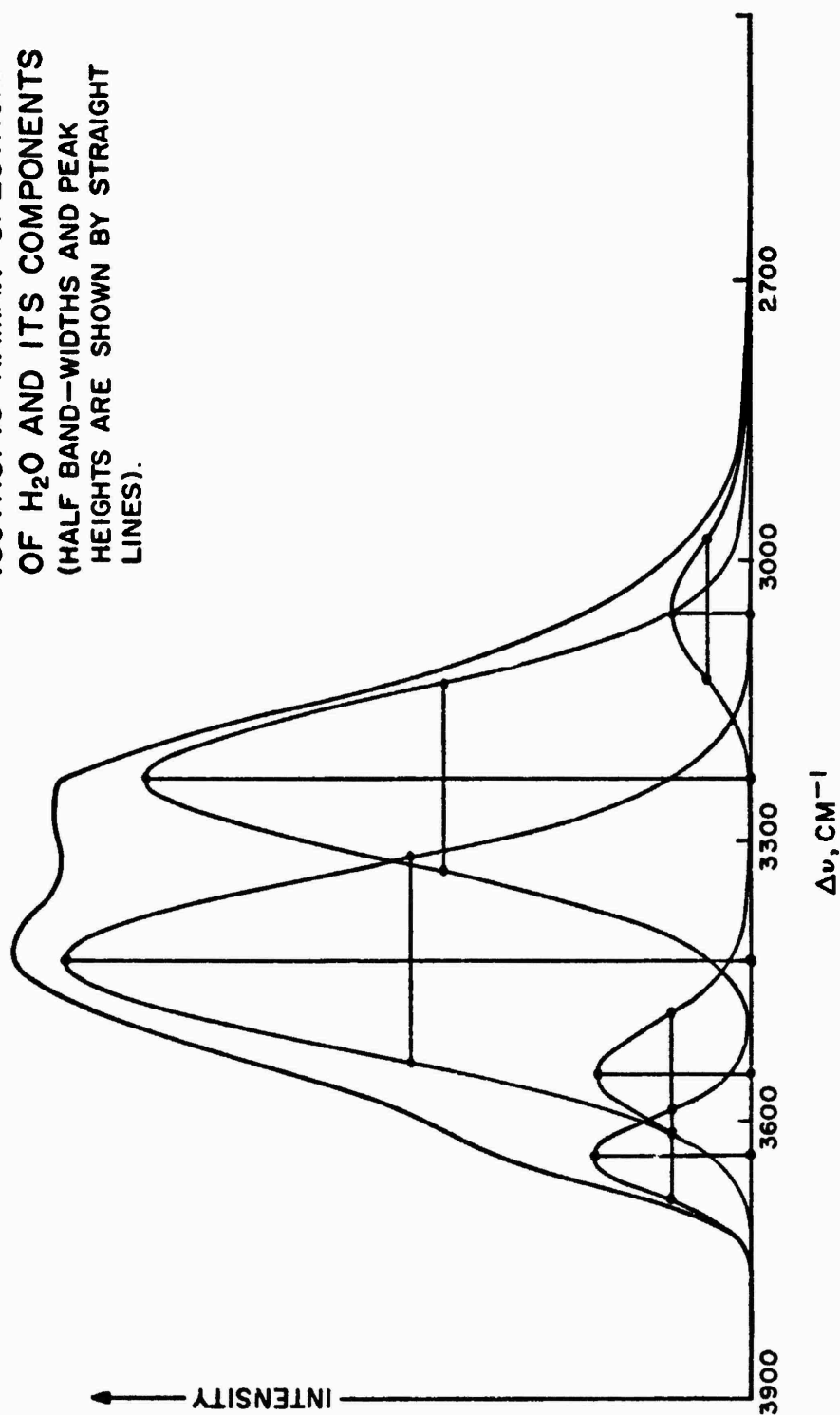


Figure 14. Isotropic Raman Spectrum of H_2O .

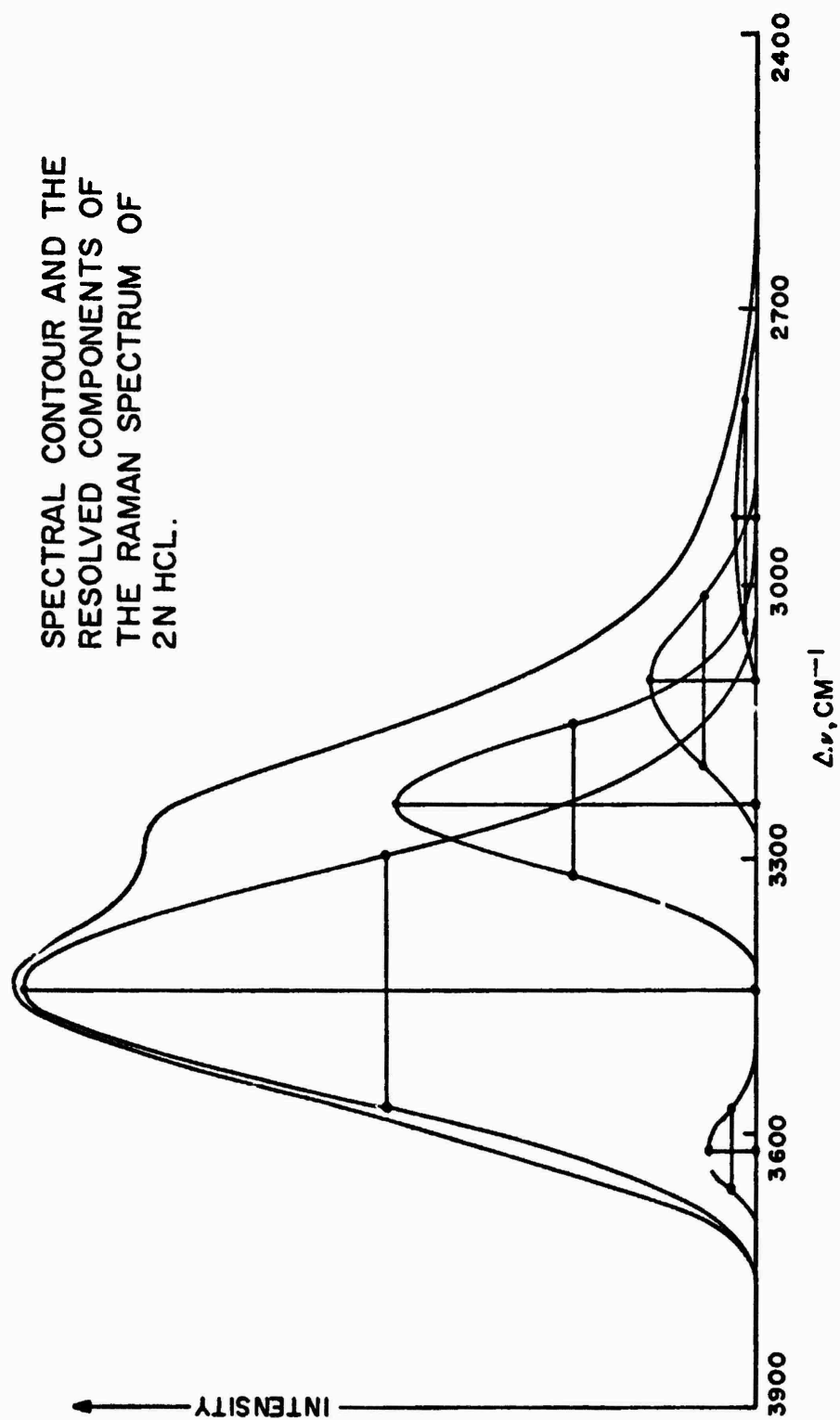


Figure 15. The Raman Spectrum of 2N HCl.

3.3 Results and Discussion

As noted in previous reports, a number of changes occur upon addition of acids to water. Of these, the two most noticeable ones are: the change in relative intensities of the components at 3225 cm^{-1} and 3415 cm^{-1} and between the trailing component at 2925 cm^{-1} and 3225 cm^{-1} band. A pictorial representation of the 3225 cm^{-1} to 3415 cm^{-1} relationship is shown in Figure 16. Figure 17 shows the same results in a graphic manner. Plotted in Figure 18 are the relative intensities of $2925/3225\text{ cm}^{-1}$ components in HCl vs. concentration. It should be noted that the relative position of the person doing the curve fitting with respect to the experimental spectrum and to the curve resolver display can cause some errors. These are estimated to be in the range of about $\pm 1\%$ and are indicated by vertical lines.

Relationship between the relative intensities, I_{2925}/I_{3225} and concentration is found to be nearly linear. The slope of the line, given by the general equation $y = mx$, is independent of the nature of the acid. The slight deviation at high concentration (6N) may be due to a small shift in the hydronium ion frequency.

The variation of the relative intensities of the two most intense components, at 3225 and 3415 cm^{-1} with respect to concentration is also found to be approximately linear. The slopes of these lines, however, depend upon the nature of the ionic species. These different slopes have been explained in terms of the solution water interactions and, furthermore, indicate that both cations and anions are responsible for these variations. Actual dependence below 0.5 N is, however, found to be nonlinear, indicating an off-balance between different perturbing effects at such concentrations.

3.4 Applications

Figures 17 and 18 provide a direct measure of the concentration of the hydronium ions present in aqueous solutions. In fact, results obtained from one of these figures can be used for independent verification of those obtained from the other.

In mixtures containing a known salt and an acid, curves of Figures 17 and 18 (used together) can provide quantitative analyses of both the components. If one of the components happens to have at least one polyatomic ionic species then the above procedure can be used in conjunction with the intensity measurements of the characteristic Raman band.

All the compounds, considered in this study, are known to be fully dissociated at the investigated concentrations. Addition of salts can, however, suppress the dissociation equilibrium of the acids towards the left, decreasing the concentration of hydronium ions.

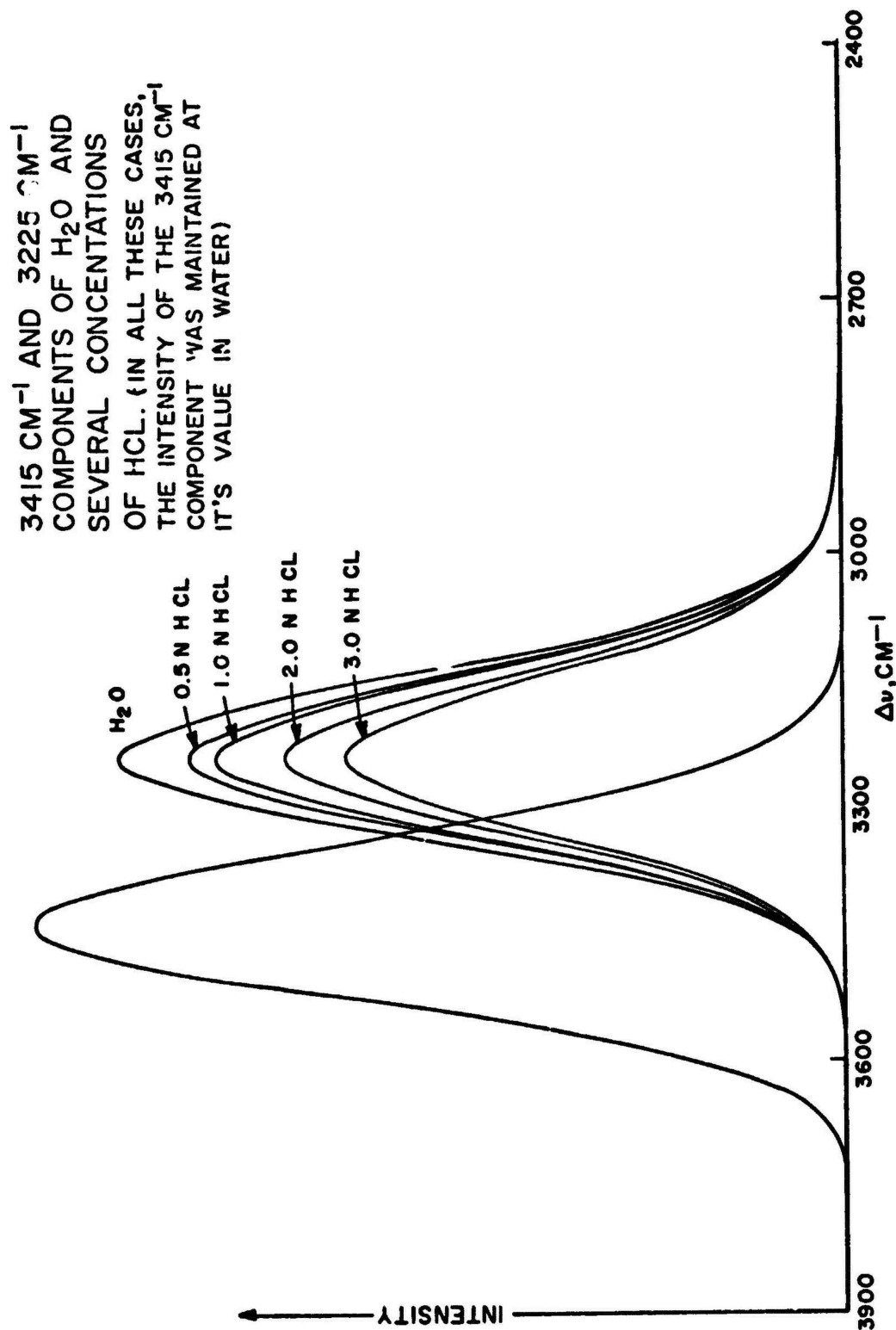


Figure 16. Specific Components of H_2O and HCl .

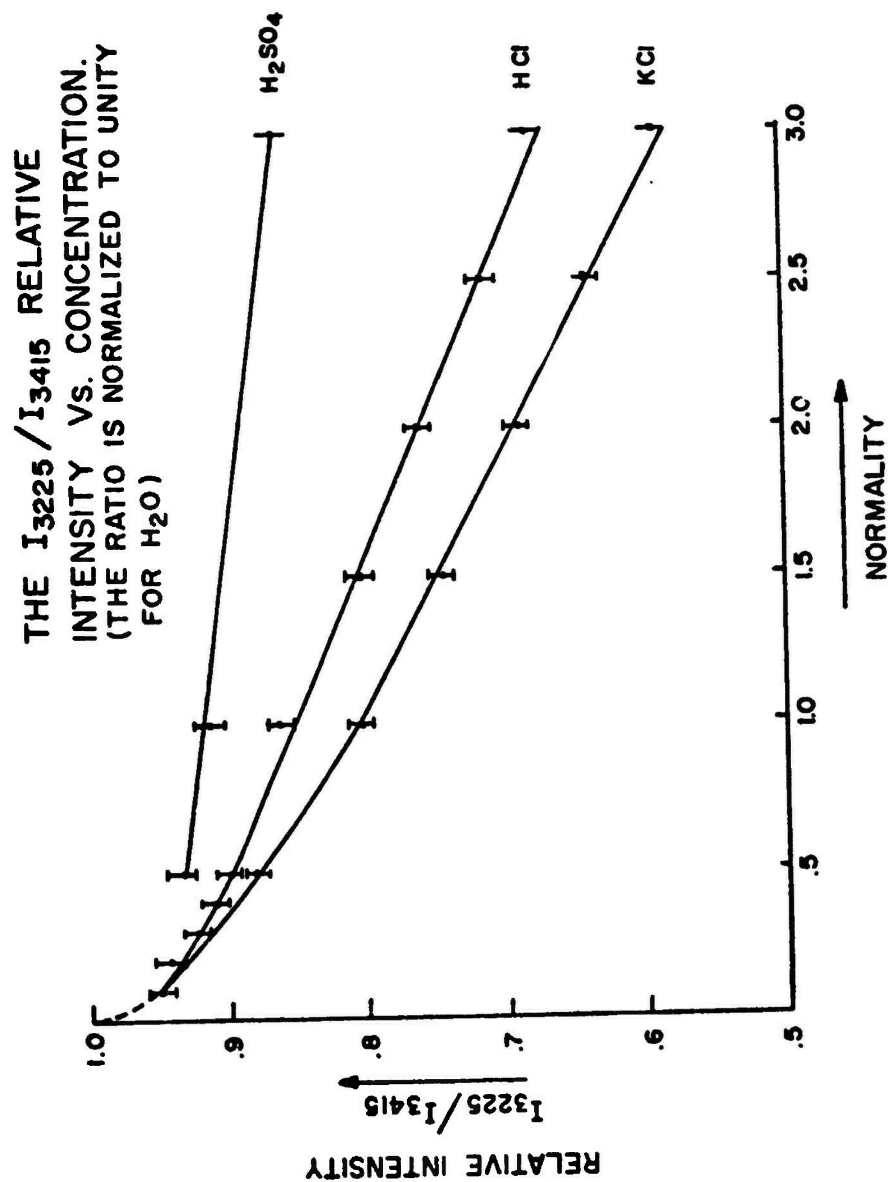


Figure 17. Relative Intensity Vs. Concentration.

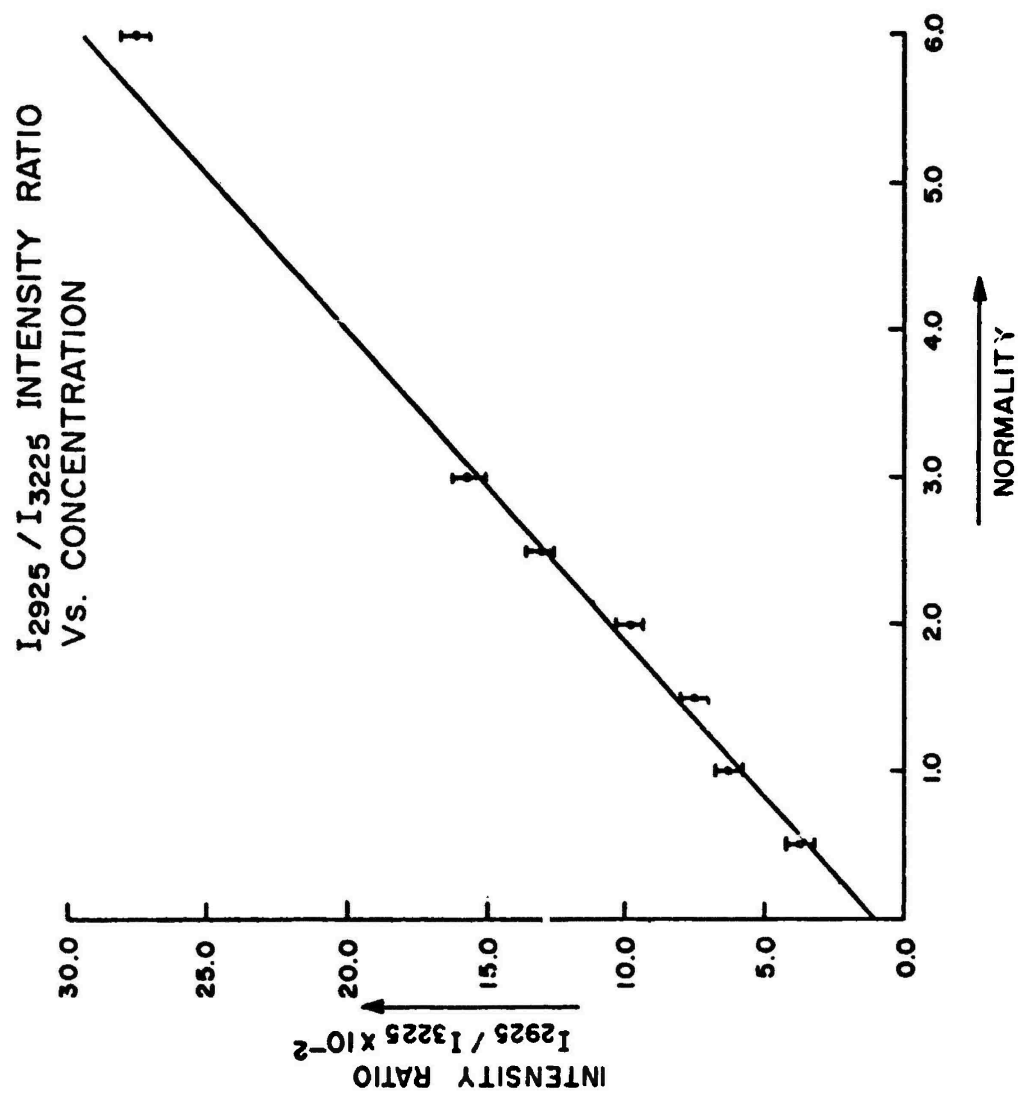


Figure 18. Intensity Ratio Vs. Concentration.



(2-1)

Studies of the equilibrium concentrations can then provide the equilibrium constants of the acids.

One of the advantages of this procedure is that it does not require the use of internal or external references. Figure 17 shows a sharp decrease in relative intensities at low concentrations. This can be very useful for qualitative and semiquantitative measurements of very small amounts of the solute, e.g., 100 ppm of HCl can be detected very easily at lower sensitivities.

3.5 Suggested Improvements

The exact relationship between relative intensities and concentration is strongly dependent upon the deconvolution procedure. Slight changes in band widths and band positions can affect the slopes remarkably. It is, therefore, necessary to use the same set of functions for the unknowns and the standards. The accuracy of determinations can be improved manyfold with the use of a computer program written so as to give best fit to the data in a least-squares sense.

The slope of the overall band, and hence of the underlying functions, depends upon the instrumental parameters and, probably, also upon the wavelength of the exciting line. The former can be eliminated by using either the same set of instrumental parameters or applying suitable corrections to the data. Change in the exciting line may lead to preferential resonance enhancement of one component compared to the other. Strong mixing of the wave functions due to Fermi resonance or/and intermolecular coupling may further complicate the problem. The first absorption band of water, due to non-bonding molecular orbital, occurs at 983 Å in the gaseous state. Removal of this from the liquid would be followed by large perturbations in the relative number of H-bonded and non-H-bonded species. The effect would be more pronounced for exciting lines close to the absorption maximum. This effect has, however, not been explored and is expected to be very small, if any, for the 4880 Å line. For wavelengths close to the maximum, it may be necessary to calibrate the curve for the particular exciting line.

Figures 19 and 20 show the ability of the Raman approach to quantify aqueous aerosols. Figure 19 is the isotropic Raman spectrum of a pure water aerosol. It looks very much like the liquid Raman spectrum (Figure 14) of water. Figure 20 is the isotropic Raman spectrum from a 6N HCl aerosol. It looks very much like the 6N liquid HCl spectrum (Figure 8).

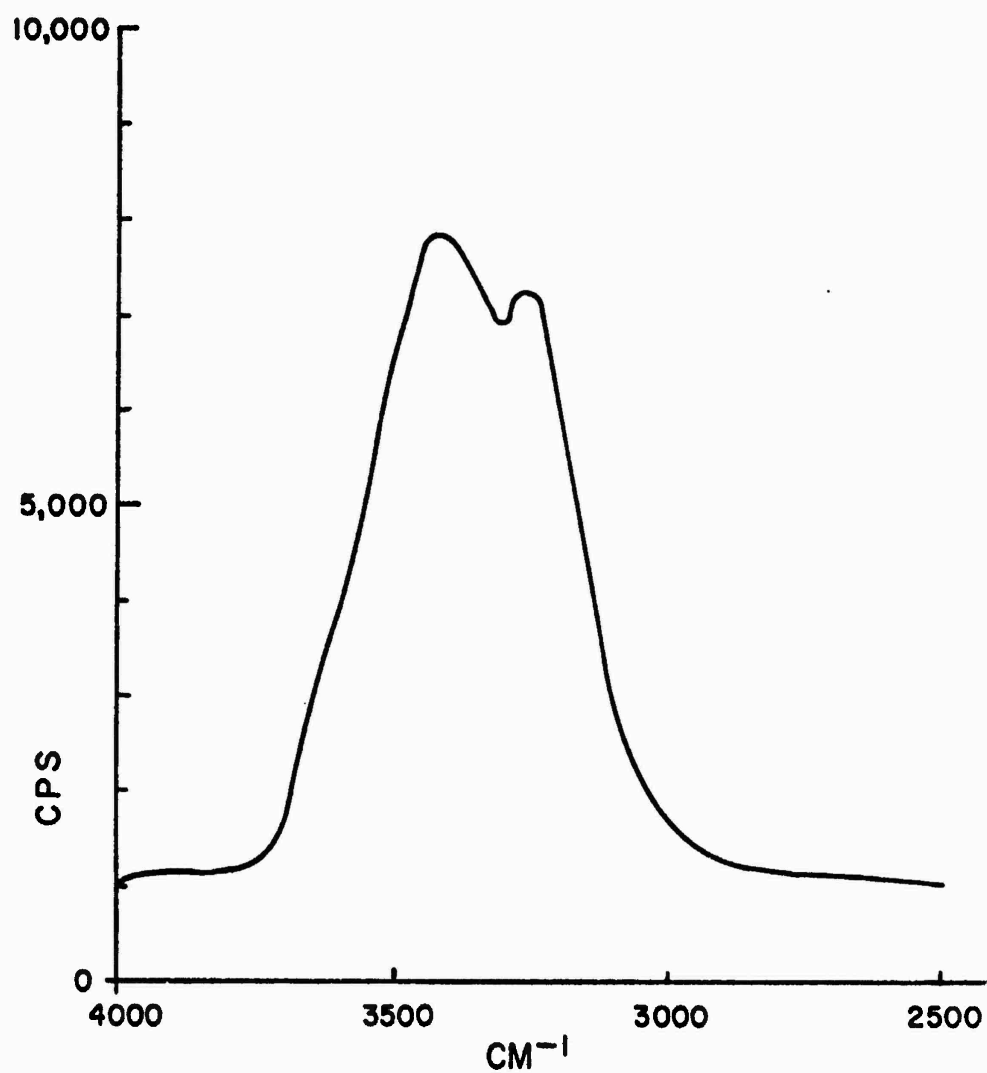


Figure 19.
RAMAN SPECTRUM OF H₂O AEROSOL

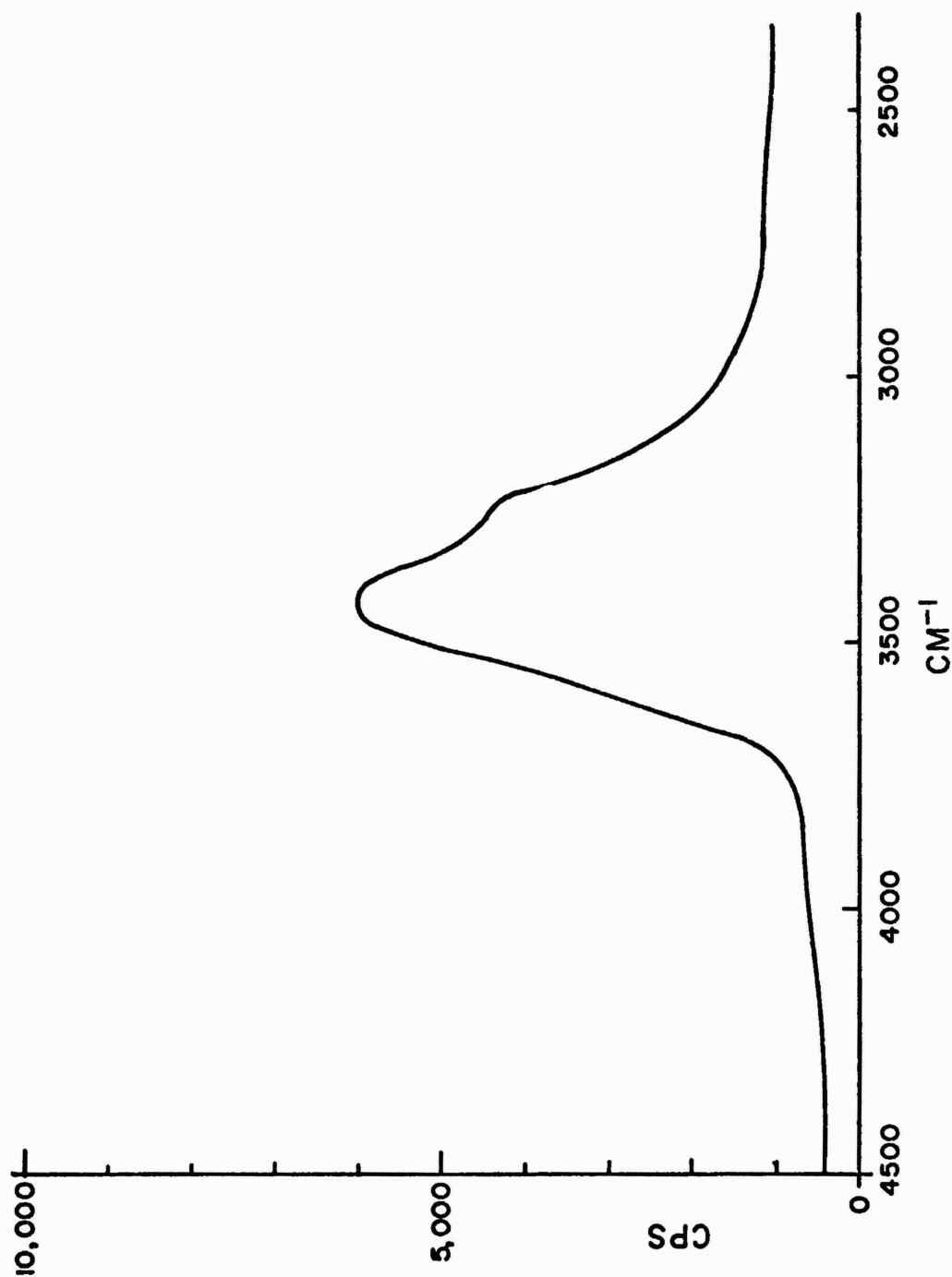


Figure 20.
RAMAN SPECTRUM OF 6N HCl AEROSOL

SECTION IV

ANALYSIS AND REVIEW

4. SUMMARIZATION OF PROBABILITY OF DETECTION MATERIALS OF INTEREST

4.1 Structure of the Hydrated Protons

Although, in the strictest sense, it is not necessary to know the structure of H_3O^+ for remote HCl detection, this information is surely useful for validating the Raman approach for this application.

4.2 H_3O^+ : Hydronium Ion

The structure of H_3O^+ has received considerable experimental (7-9) and theoretical (19,20) attention because of its importance in acidic solutions. Most of the experimental information results from measurements in the solid state whereas NO calculations exist for isolated H_3O^+ and some of its solvated species. Both experiments and involved theoretical calculations (employing polarization functions and larger basis sets) support a nearly flat pyramidal structure with OH bond lengths of $\sim 1.02 \text{ \AA}$ and an HOH angle of 115° (Figure 21). The barrier to inversion is estimated to be 2-3 K cal/mole compared to a value of 5.8 for the isoelectronic NH_3 molecule.

Molecular reorientations in crystalline hydrates produce considerable distortions of the structural parameters. Almlöf and Wahlgren (21) examined the effects of neighboring electrostatic fields on the structure of H_3O^+ ion. A nearby negative charge was found to increase the OH distance and decrease the HOH angle to make O-H-X as nearly linear as possible. Downward shift of the ν component of H_2O also suggests reorientation of the water molecule in presence of ions. Broadness of the bands in solution along with the bands due to the solvent, however, does not permit an evaluation of the average configuration in the liquid state.

4.3 H_5O_2^+ : Bihydronium Ion or Bioxonium Ion*

Following its detection in dihydrates of strong acids, a

(21) J. Almlöf and V. Wahlgren, Theoret. Chim. Acta 28, 161, (1973).

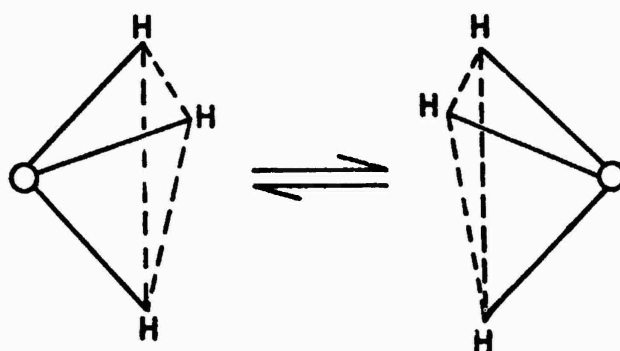


Figure 21.
PROPOSED STRUCTURE FOR H_3O^+

number of X-ray (22-24) neutron diffraction (25) and vibrational (26,27) studies have been reported. It is found to have C_{2h} structure linked to surrounding anions by four nearly equal H-bonds of 2.78-2.79 Å. The O-H-O distance is estimated as 2.4-2.5 Å; proton being at or near the center (Figure 22). The O-H bonds at each end can be cis, trans or gauche with respect to each other, and all three arrangements have been observed. Apparently, the overall attainment of minimum energy in the crystal lattice is influential in determining the $H_5O_2^+$ structure that is found. No indication has been found for the existence of the monohydrate of the hydronium ion $H_3O^+ \cdot H_2O$.

Pavia and Giguère (26) assigned the vibrational spectra of $H_5O_2^+$ in terms of the trans configuration of C_{2h} symmetry (Figure 23). Bands at 1700, 412, and 1080 cm^{-1} were assigned to anti-symmetric stretching, symmetric stretching, and bending modes, analogous to those of HF at 1500, 600 and 1250 cm^{-1} . The O-H frequency at 1700 cm^{-1} is also consistent with the short H-bond (Figures 24 and 25).

No definite answer is available to the question whether $H_5O_2^+$ exists as a discrete entity in the liquid state. The vibrational spectrum near the concentration of dihydrate (50.34%) is similar to that at lower and higher concentrations. In the absence of the crystalline force field, the solute could very well be the hydrated hydronium ion $H_3O^+ \cdot H_2O$.

4.4 $H_7O_3^+$

No experimental evidence exists for the presence of this species in liquid or solid hydrates. X-ray diffraction results of $HCl \cdot 3H_2O$ at -190° indicate that the trihydrate exists as $H_5O_2^+ Cl^- \cdot 2H_2O$. A similar study on the nitric acid trihydrate gave evidence for the presence of $H_3O^+ \cdot NO_3^- \cdot 2H_2O$ species. CNDO/2

-
- (22) J. O. Lundren and I. Olovsson, *Acta Cryst.*, 23, 966, (1967).
 - (23) *Ibid.*, 23, 971, (1967).
 - (24) I. Olovsson, *J. Chem. Phys.*, 49, 1063, (1968).
 - (25) J. M. Williams, *Inorg. Nuc. Chem Letters*, 3, 297, (1967).
 - (26) A. C. Pavia and P. A. Giguère, *J. Chem. Phys.*, 52, 3551, (1970).
 - (27) R. D. Gillard and G. O. Wilkinson, *J. Chem. Soc.*, 1640, (1964).

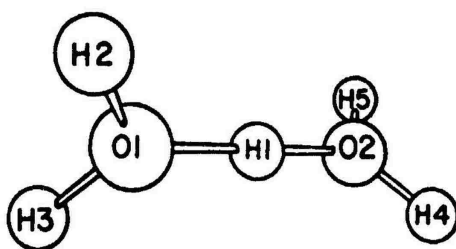


Figure 22.
PROPOSED STRUCTURE FOR H_5O_2^+

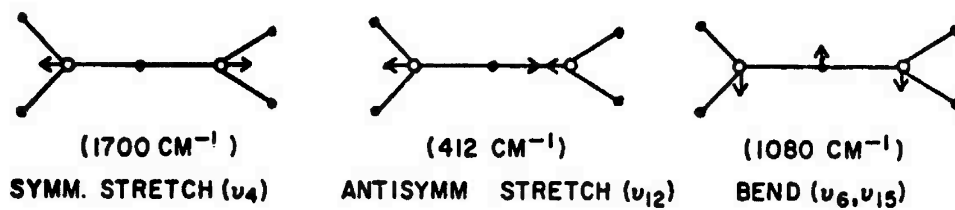


Figure 23.
 SCHEMATIC PRESENTATION OF
 VIBRATIONAL SPECTRUM OF H_5O_2^+

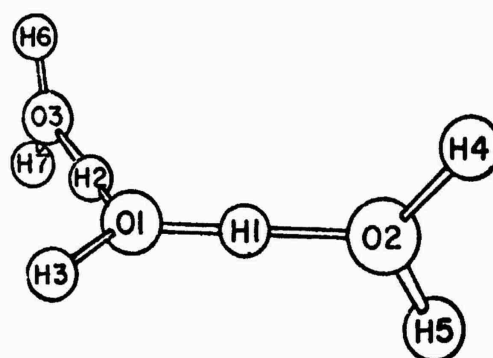
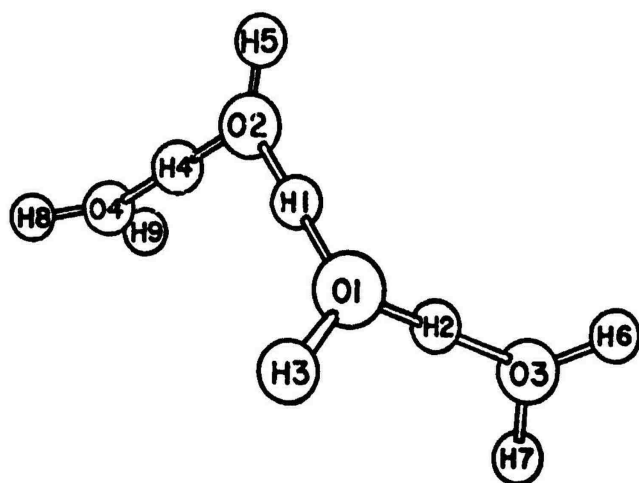
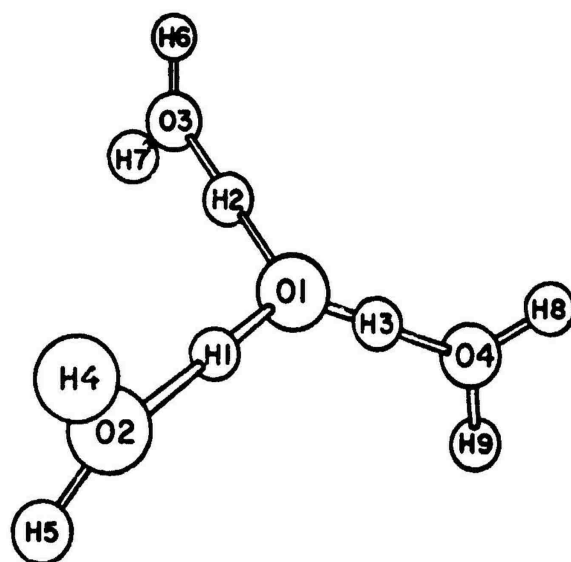


Figure 24. .
 PROPOSED STRUCTURE FOR H_7O_3^+



(a)
CHAIN TYPE



(b)
EIGEN TYPE

Figure 25.
PROPOSED STRUCTURES FOR H_9O_4^+

calculations *(28) suggest slight stability for these species with a chain type structure as shown in Figure 24.

4.5 H_9O_4^+

There is evidence that in solution H_3O^+ binds other water molecules fairly strongly, presumably attracting an oxygen atom to each of its rather positive hydrogen atoms. Rudolph and Zimmerman (29) interpreted the infrared of the tetrahydrate of HBr at -170° in terms of the species $\text{H}_9\text{O}_4^+ \cdot \text{Br}^-$.

Semi-empirical theoretical calculations favor the open structure more than the cyclic, and two different structures (as shown in Figures 25a and 25b) are found to have nearly the same stability. The chain structure is, however, more consistent with mobilities of H and OH ions in aqueous solutions.

Now evidence is accumulating that in liquid water H_3O^+ is certainly not the only and perhaps not the most common form. Recent crystal structure determinations supply some important facts in this problem. Experimental data indicates there is no preference for H_3O^+ when there are enough water molecules to permit higher protonic ions to form.

(15) Theoretical calculations and mass spectrometric measurements indicate that there is no unique choice of n for which the stability of $\text{H}^+n\text{H}_2\text{O}$ dominates the stability for other choices of n. It may thus be inferred that the correct picture in acid solutions may comprise a statistical distribution of the various basic structures discussed above.

* CNDO/2 = A molecular orbital calculation with complete neglect of differential overlap, phase 2.

(28) M. DePaz, S. Sherrerson, and L. Friedman, J. Chem. Phys., 52, 3362, (1970).

(29) J. Rudolph and H. Zimmerman, Z. Physik Chem., 43, 311, (1964).

SECTION V

CONCLUSIONS

5. GENERAL

5.1 Results. All of the objectives of the present program have been met or exceeded. A technique has been developed, utilizing the principles of Raman spectroscopy, whereby it is possible to measure total acidity in any background matrix including water. From laboratory data it can be shown that:

(a) Aqueous acid aerosols and solutions can be indirectly analyzed using Raman methods by assessing the effect that the acid has on the structure of the water matrix.

(b) Remote detection of total atmospheric acidity should be possible under the conditions discussed in Appendix B.

The approach developed is applicable to all acid systems, including aqueous HCl solutions where neither the cation or anion contain a chemical bond.

5.2 Direct Measurement of the Hydrated Proton. Under this program no direct Raman spectrometric technique for measuring the hydronium ion and other hydrated protons $[H(H_2O)_n]^+$ was found. Detailed Raman spectra were measured for aqueousⁿacid solutions over the frequency region 10 cm^{-1} to 4500 cm^{-1} . Several acids were investigated, including HCl, at a variety of concentrations from 0.25N to 6N. No spectral lines were observed which could be assigned to the hydrated proton. The next step, therefore, was to look for indirect measurement possibilities.

5.3 Acid Effects on the Structure of Water. When an acid is added to water there is an obvious change in the shape of the broad Raman band centered at $\sim 3450\text{ cm}^{-1}$ and assigned to the symmetric OH stretch, ν_1 . This change is of sufficient magnitude that it is visually observable. For the purposes of this investigation, the pure water band was deconvoluted into five (5) Gaussian curves. The two (2) largest of these curves are centered at 3225 cm^{-1} and 3415 cm^{-1} . When acid is added to the water, and the same Gaussian curve fitting procedure is used, six (6) curves are required to meet the deconvolution criteria. The new curve, centered at 2925 cm^{-1} has been tentatively assigned to H_3O^+ (and other hydrated protons). The curve at 2925 cm^{-1} is required only when acid is added. The spectra from salt solutions (NaCl, KCl, Na_2SO_4) do not require this sixth curve for proper deconvolution. The salt does, however, affect

the curve at 3225 cm^{-1} . From the data it can be concluded that ratioing the intensities of the 2925 cm^{-1} curve to the 3225 cm^{-1} curve gives acid concentration. Ratioing the line at 3225 cm^{-1} to that at 3415 cm^{-1} (held to its value in water) can give both acid (if background salt concentration is known) and salt concentration. Use of all three (3) curves gives unambiguous measurement of both acid and salts without a previous background measurement being required. Thus a method of identifying and quantifying aqueous acid aerosols and solutions has been developed and the program objectives have been met.

5.4 Remote Detection. The remote detection of aqueous acids depends on having Raman cross sections which are sufficiently large to give the required sensitivity and range. Cross sections for the 2925 cm^{-1} , 3225 cm^{-1} and 3415 cm^{-1} lines have been determined to be $2.4 \times 10^{-28}\text{ cm}^2\text{ molec}^{-1}$ (13N HCl), $5.6 \times 10^{-28}\text{ cm}^2\text{ molec}^{-1}$ (H_2O) and $6.7 \times 10^{-28}\text{ cm}^2\text{ molec}^{-1}$ (H_2O) respectively. Using the smallest cross section ($2.4 \times 10^{-28}\text{ cm}^2\text{ molec}^{-1}$), a table of minimum detectability vs. range has been generated as shown in Appendix B. From this table it is possible to determine the applicability of the remote Raman technique to an acid detection and/or quantification problem.

SECTION VI

RECOMMENDATIONS

6. GENERAL

6.1 Future Action. Inasmuch as it has been demonstrated in the laboratory that aqueous acid aerosols and solutions are indirectly measureable by Raman techniques, it is now possible to address an Air Force need - remote acid detection and quantification. These are three (3) steps to attaining this goal:

(a) The degree to which the water band shape must be defined for reliable remote analysis must be ascertained.

(b) Preliminary remote acid measurements should be made on an extant remote Raman spectrometer equipped with a monochromator.

(c) A remote Raman spectrometer specifically designed for remote acid detection and compatible with the Air Force mission, should be constructed and tested.

When these three (3) milestones are met, the Air Force will have an operational acid detector.

6.2 Water Band Shape. Investigations to date have utilized the total water curve for acid analysis. In remote sensing, getting the complete shape of the water-acid band may be impractical. It is, therefore, necessary to assess how many actual points on the curve are required for aqueous acid analysis and the most practical way of obtaining this data under operational conditions.

6.3 Preliminary Field Tests. It is desirable to perform some preliminary remote aqueous acid measurements so that the information gleaned can be used to help design an optimized remote system. There is an operational remote Raman system at Edgewood Arsenal, Maryland suitable for these measurements. This instrument is equipped with a motorized polychromator capable of obtaining Raman band shapes. This instrument is presently being equipped with computerized data handling so that deconvolution and ratioing can be fully automated. In addition, a remote (400 meter) sample cell is available into which aqueous acid aerosols can be injected. Wet chemistry can then be used to check the aerosol for acid content and for calibrating system performance. Of particular interest, besides confirming the sensitivity vs. range calculations, is the scattering effects from the aerosol itself and the instrumentation necessary to overcome these. When the experimental data, the calculated

performance and the projected instrument design are all congruous, then a new remote Raman system should be built.

APPENDIX A

RESEARCH LABORATORY RAMAN SPECTROMETER

1. Basic Raman Laboratory Spectrometer

The Block Engineering modular laboratory Raman spectrometer was used to make the measurements reported herein. This unit may be set up in several configurations so that the highest quality data output can be obtained. This instrument has all of the basic components common to photoelectric Raman spectrometers. These include:

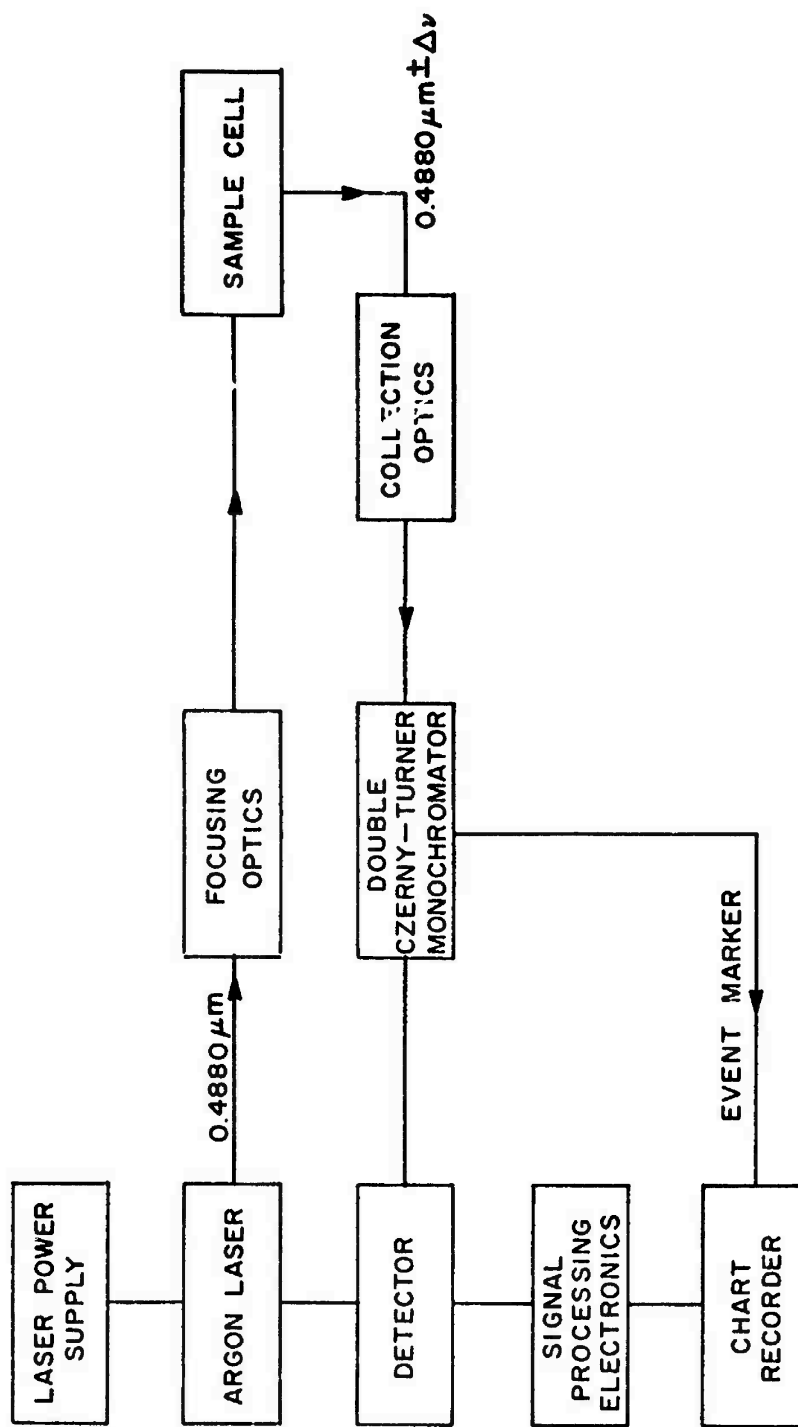
- (a) Intense monochromatic light source,
- (b) Sample volume or cell,
- (c) Raman scattering collector,
- (d) Spectral discriminator,
- (e) Detector,
- (f) Signal processor and
- (g) Data display.

The basic Raman spectrometer used for these measurements is shown diagrammatically in Figure 26. The argon laser used is a Spectra-Physics Model 165-03 which can be adjusted to emit several lines and has its strongest emissions at 0.4880 μm and 0.5145 μm . In addition, continuous wavelength coverage in the visible region (0.5750 μm to 0.6350 μm) is available by inserting a dye laser between the argon laser and the focusing optics, (Figure 27). Best results for the experiments run during this program were obtained using 0.4880 μm irradiation and all of the data shown was taken using this condition.

The sample cell used for the liquid acid measurements was a standard cuvette such as used in ultraviolet and visible absorption spectroscopy. A special device, which is described in Section 1.2, was used to make the aerosol measurements.

The spectral sorter is a commercially available Jarrell-Ash 1-meter double monochromator. This unit has excellent stray light rejection and high linear dispersion.

The detector is a high quantum efficiency cooled photomultiplier tube. The output of this tube is amplified by photon counting electronics (for maximum sensitivity). The processed signal is displayed on the chart recorder as a plot of intensity vs. wavelength as the spectral sorter scans through the frequency region of interest.



BLOCK DIAGRAM OF RAMAN SPECTROMETER

Figure 26.

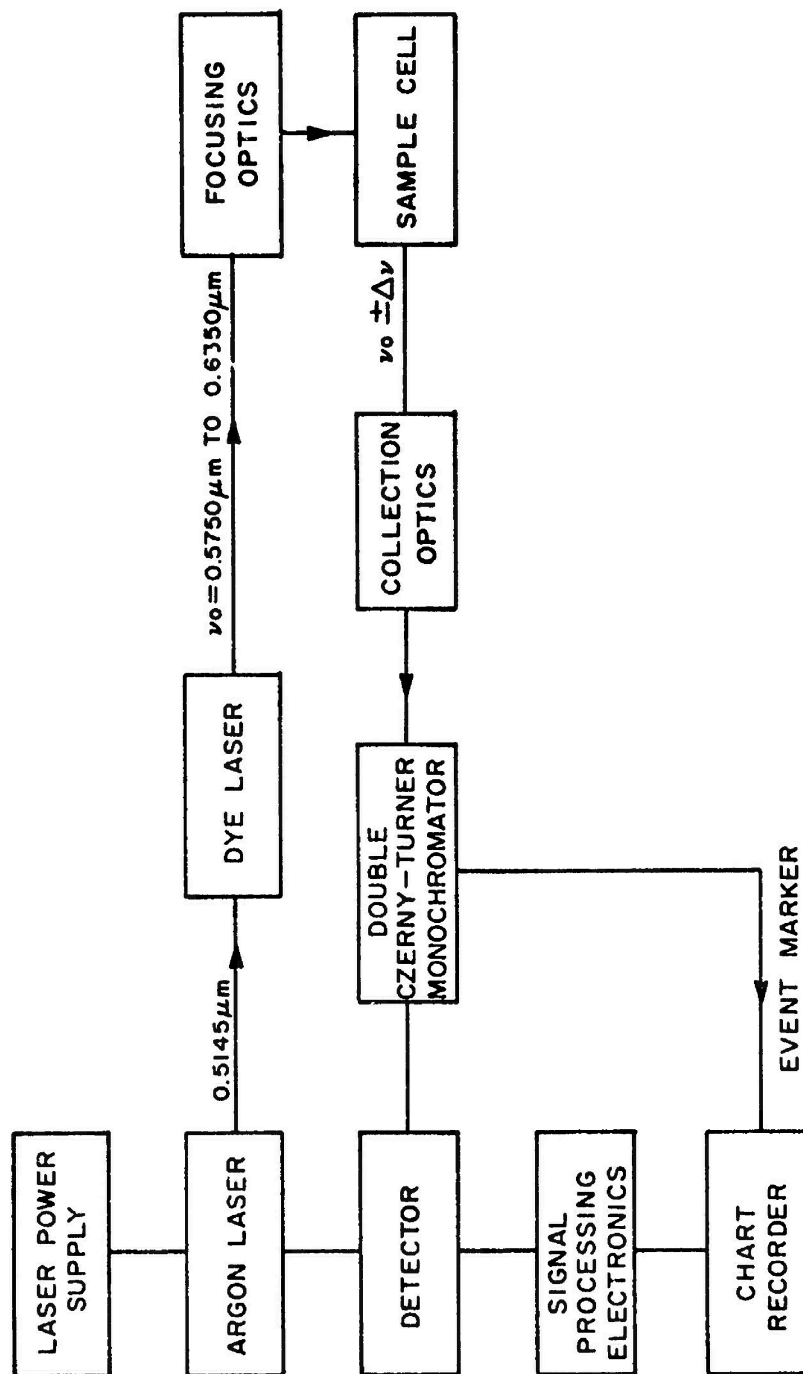


Figure 27.

BLOCK DIAGRAM OF RAMAN SPECTROMETER (WITH DYE LASER)

1.1 Instrument Calibration

In this program, where Raman spectra are used for qualitative and quantitative analysis, it is important to know accurately the operating parameters of the spectrometer used. For that reason the Block Raman instrument is very carefully calibrated.

Instrument calibration consists of:

- (a) Determining the amount of interference from the plasma lines of the laser,
- (b) Evaluating the interference filter which is used to reject unwanted laser lines,
- (c) Determining stray light rejection of the double monochromator,
- (d) Determining aberrations in the monochromator,
- (e) Determining accuracy and reproducibility of the wavelength scale,
- (f) Measuring performance of the photomultiplier tube and
- (g) Checking Poissonian behavior or quantum counting noise.

The above calibrations are performed several times during the course of a one-year program. This is required because filters degrade, cams and screws wear, photomultiplier tubes age, etc.

1.2 Aerosol Cell

In order to determine whether the data obtained for aqueous acid solutions is comparable with that for aqueous acid aerosols, it was necessary to construct a cell in which the liquid droplets of controlled size could be generated. The aerosol was produced by using an atomizer with an adjustable head. Droplet size could be controlled reasonably well by either the head adjustment or by the pressure of nitrogen gas used to drive the sprayer. The atomizer head was inserted through a quartz tube (near the top) whose diameter was such that the end of the spray reach the opposite wall of the tube. This was done so that excess condensed liquid would run down the tube rather than get into the field-of-view of the Raman laser beam. A reservoir was placed at the bottom of the tube to collect the spent acid. Fresh acid was always used in the atomizer. Raman scattering was obtained from many portions of the aerosol cloud by raising or lowering the tube. 180° observation angle was used to measure several acid concentrations between 2N and 6N. The data taken using this cell could easily be related to that for the aqueous solutions.

APPENDIX B
Sensitivity Calculations for the Remote Detection
of Aqueous Acid Clouds

1.0 Remote Raman Parameters

The following terms, necessary for calculation of the sensitivity of a remote Raman spectrometer as a function of distance, are given in this section:

- (a) Parameters for a remote Raman spectrometer,
- (b) Terms for calculating loss of signal due to the atmosphere and to background,
- (c) Characteristics of an aqueous acid cloud, and
- (d) Operational considerations.

1.0.1 Remote Raman Spectrometer

The parameters of a remote Raman spectrometer presented herein are both realizable and implementable. They represent an up-graded version of a Block Engineering built system presently in daily operation (Edgewood Arsenal).

D = diameter of the optical collector = 91 cm

T_E = transmitter efficiency = 0.93

T_R = receiver efficiency = 0.20

Q_E = detector quantum efficiency = 0.46

E = laser energy per pulse = 1 J

p = laser pulse repetition rate = 1 pps

λ_0 = laser wavelength = 0.3472 μm

V = receiver field-of-view = 10^{-6} st.

$\Delta\lambda$ = system bandwidth = 2×10^{-4} μm

1.0.2 Atmospheric and Background Considerations

Raman signal transmission losses due to atmospheric absorption are a major consideration when calculating remote detectability. Terms of interest are:

σ = atmospheric attenuation coefficient = 2.88×10^{-6} cm^{-1} .

R = range (from instrument to sample) = (variable) cm.

A second loss is due to background spectral radiance. As the following constants show, there is a much greater effect during

the day:

$$B_{\lambda_D} = \text{daytime spectral radiance} = 2 \times 10^{-4} \text{ W cm}^{-2} \text{ st}^{-1} \mu\text{m}^{-1}.$$

$$B_{\lambda_N} = \text{nighttime spectral radiance} = 10^{-8} \text{ W cm}^{-2} \text{ st}^{-1} \mu\text{m}^{-1}.$$

1.0.3 Aqueous Acid Clouds

The Raman cross-section for the Gaussian curve assigned to hydronium ion (H_3O^+) has been measured. In addition, information is known about acid cloud size. The needed terms are:

$$\ell = \text{length of range gate (smaller than cloud diameter)} = 10^4 \text{ cm.}$$

$$X_R = \text{Raman } 180^\circ \text{ cross-section} = 2.4 \times 10^{-28} \text{ cm}^2 \text{ molecule}^{-1}.$$

$$\lambda_R = \text{Raman return wavelength} = 0.3879 \text{ nm.}$$

1.0.4 Operational Considerations

Finally, there is the question of how long it is practical to perform a measurement, and what signal to noise ratio is required. Here:

$$t = \text{analysis time} = 60 \text{ sec.}$$

$$\text{SNR} = \text{signal to noise} = 3.$$

1.1 Pertinent Equations for Sensitivity Calculations

There are three (3) pertinent equations for calculating the sensitivity of a particular remote Raman spectrometer to detection of a specific species. (*)

$$\text{SNR} = \frac{F_R \sqrt{N}}{\sqrt{F_R + F_B}} \quad (1-1)$$

$$F_R = C(9.2 \times 10^{36} D^2 T_E T_R Q_E E \lambda_o \ell X_R) \cdot \frac{\ell^{-2\sigma_R}}{R^2}, \quad (1-2)$$

and

$$F_B = 2.64 \times 10^8 B_\lambda \ell D^2 V \Delta\lambda T_R Q_E \lambda_R \quad (1-3)$$

* A detailed derivation of these equations is available from Block Engineering, Inc.

where terms not previously defined

N = number of laser pulses = t_p = 60 pulses

F_R = Raman photoelectrons collected from a single pulse

F_B = Background photoelectrons collected during measurement
of F_R

C = Sample concentration = variable parts (1 part = 100%,
 10^{-6} part = 1 ppm).

Inasmuch as the minimum detectable C as a function of R is
of interest, after substitution of the given values, equation
(1-2) may be written:

$$\frac{F_R}{C} = 5.43 \times 10^{15} \frac{l^{-2}\sigma R}{R^2} \quad (1-4)$$

and

$$F_{B_D} = 3.11 \times 10^1 \quad (1-5)$$

where

F_{B_D} = Background photoelectrons collected during
daytime measurement of F_R .

For nighttime measurements,

$$F_{B_N} = \text{negligible.} \quad (1-6)$$

It is now possible to calculate the minimum detectable C
(for a SNR of 3 and $t = 60$ sec.) for various ranges. The neces-
sary calculations are shown in Table 1.

TABLE I
TABULATION OF MINIMUM DETECTABLE H_3O^+ (HCL) VS. RANGE

| R , cm | R^2 cm ² | $\frac{1-2\sigma R}{R^2}$, cm ⁻¹ | $\frac{1-2\sigma R}{R^2}$, cm ⁻³ | $\frac{F_R}{C}$, photons | PPM H_3O^+ (night) | % HCL (night) | PPM H_3O^+ (day) | % HCL (day) |
|-------------------|--------------------------|---|---|------------------------------|-------------------------|--------------------|-----------------------|--------------------|
| 5×10^4 | 2.5×10^9 | 0.75 | 3×10^{-10} | 1.6×10^6 | 0.09 | 1×10^{-3} | 1.4 | 2×10^{-2} |
| 10^5 | 10^{10} | 0.56 | 5.6×10^{-11} | 3×10^5 | 0.5 | 6×10^{-3} | 7.4 | 9×10^{-2} |
| 1.5×10^5 | 2.3×10^{10} | 0.42 | 1.8×10^{-11} | 9.8×10^4 | 1.5 | 2×10^{-2} | 23 | 3×10^{-1} |
| 2×10^5 | 4×10^{10} | 0.31 | 7.8×10^{-12} | 4.2×10^4 | 3.6 | 4×10^{-2} | 53 | 6×10^{-1} |
| 2.5×10^5 | 6.3×10^{10} | 0.24 | 3.8×10^{-12} | 21×10^4 | 7.1 | 9×10^{-2} | 106 | 1.3 |
| 3×10^5 | 9×10^{10} | 0.18 | 2×10^{-12} | 1.1×10^4 | 13 | 2×10^{-1} | 200 | 2.4 |
| 3.5×10^5 | 1.2×10^{11} | 0.13 | 1.1×10^{-12} | 6.0×10^3 | 25 | 3×10^{-1} | 370 | 4.4 |
| 4×10^5 | 1.6×10^{11} | 0.10 | 6.3×10^{-13} | 3.4×10^3 | 44 | 5×10^{-1} | 660 | 7.9 |
| 4.5×10^5 | 2×10^{11} | 0.08 | 4×10^{-13} | 2.2×10^3 | 68 | 8×10^{-1} | 1010 | 12 |
| 5×10^5 | 2.5×10^{11} | 0.06 | 2.4×10^{-13} | 1.3×10^3 | 115 | 1 | 1700 | 20 |
| 6×10^5 | 3.6×10^{11} | 0.03 | 8.3×10^{-14} | 4.5×10^2 | 333 | 4 | 5000 | 60 |
| 7×10^5 | 4.9×10^{11} | 0.02 | 4.1×10^{-14} | 2.2×10^2 | 682 | 8 | - | - |



*MISSION
of
Rome Air Development Center*

RADC is the principal AFSC organization charged with planning and executing the USAF exploratory and advanced development programs for information sciences, intelligence, command, control and communications technology, products and services oriented to the needs of the USAF. Primary RADC mission areas are communications, electromagnetic guidance and control, surveillance of ground and aerospace objects, intelligence data collection and handling, information system technology, and electronic reliability, maintainability and compatibility. RADC has mission responsibility as assigned by AFSC for demonstration and acquisition of selected subsystems and systems in the intelligence, mapping, charting, command, control and communications areas.